Summer 2024

Li-ion battery resistance during external short circuits and cyclic ageing

KAYNAT ZIA
University of Texas at Arlington

Li-ion battery resistance during external short circuits and cyclic ageing

A Dissertation Presented
by
Kaynat Zia

Submitted in partial fulfillment
of the requirements for the degree of
Doctor of Philosophy
The University of Texas at Arlington
August, 2024

Supervising Committee:

Dr. Rasool Kenarangui
Dr. Ali Davoudi
Dr. Wei-Jen Lee, Supervising Professor

Acknowledgements

I am truly grateful to Dr. Wei-Jen Lee, for his guidance, patience and vision that led me to accomplish what I did in the last half a decade of my life and hence, a Ph.D.

I also extend my thanks to all my dissertation committee members, Dr. Rasool Kenarangui and Dr. Ali Davoudi for their comments and feedback.

I also thank my friends and lab mates Anusha Papasani and Po-En Su from Energy Systems Research Center (ESRC).

Lastly, I would like to thank all EE department members of UTA and Mr. Arun Nair.

Dedication

I dedicate this work to my mother, Zarqa and my father, Zia, who endured the pain of being apart from me so I could pursue my dreams.

To my Nani Nana, Zubaida and Saeed, and my siblings, (Dr.) Taimour, (Dr.) Bakht, (Dr.) Isha and Dolly, for I'd be nothing without them.

Abstract

External short circuit testing (ESCT) is one of the many steps towards ensuring lithium-ion (Li-ion) batteries are safe for different applications. The nature of testing is sensitive due to the concern of safety and data integrity. Great care and planning must be done before conducting these tests. Bouncing in recorded data is observed in literatures with high sampling rates due to switching and moving mechanical parts. This impacts the estimation accuracy of battery internal parameter values especially the effective ohmic resistance (Ro). This dissertation proposes a zero bouncing circuit design to eliminate this problem. Multi-rate Pulse Discharge Testing (MPDT) is conducted at safe current levels up to 7C at 25°C. To extract the values of internal battery parameters, Python is used, and the values are compared with those from an ESCT conducted using the same setup. In a bid to prevent more batteries from entering the waste stream, internal resistance of a post external short circuit battery (PESCB) is measured and compared to the internal resistance change during cyclic ageing of a healthy battery (HB). The data collected and results will be used to assess the reusability of lightly abused batteries based on their internal resistance change.

Contents

Table of figures

Chapter 1: Introduction

Electrical safety

Electrical hazards and safety are major concerns in today's society, with significant socioeconomic impacts. Deniers of global warming often capitalize on disasters linked to modern, cleaner energy options. Electrical safety involves a comprehensive range of precautions and practices designed to mitigate risks associated with electrical systems.

In residential settings, a primary concern is the safety of wiring and installation. Faulty wiring, inadequate insulation, and overloaded circuits pose significant hazards. To prevent electrical fires and shocks, it is essential to ensure proper installation by qualified electricians, use appropriate wiring materials, and conduct regular inspections.

In industrial environments, electrical safety extends to addressing potential hazards related to electrical equipment and machinery. Workers face risks such as electrical shock, arc flashes, and explosions. Crucial measures include adherence to lockout/tagout procedures, which involve isolating energy sources before maintenance or repairs. Implementing robust training programs, providing personal protective equipment (PPE), and conducting routine equipment inspections are vital components of industrial electrical safety.

International organizations, such as the International Electrotechnical Commission (IEC) in Europe and the National Electrical Code (NEC) in the United States, play a key role in developing and updating electrical safety standards. These standards evolve in response to technological advancements, emerging risks, and lessons learned from incidents. Adherence to these standards helps create safer environments, reduces electrical accidents, and fosters a culture of responsible electrical practices.

Electric arcs are a particularly dangerous phenomenon where the air between two conducting bodies becomes ionized, allowing current to flow through the air and forming a visible arc. The electric arc can cause explosions, equipment damage, casualties, and severe injuries. While proper equipment maintenance, wiring, and regular checkups can prevent electric arcs, they can sometimes be inevitable, such as during circuit breaking and closures. The arcing current is usually less than the bolted fault current due to the resistance of the ionized air. Accurate knowledge of bolted fault current and arcing current values is essential to set up proper protection against arcing.

Lithium-ion batteries

In the late 1970s, American chemist John B. Goodenough and his research team made a groundbreaking discovery, showcasing the potential of rechargeable Li-ion batteries. Their innovative work, particularly in the use of lithium cobalt oxide as a cathode material, laid the groundwork for the commercialization of Li-ion batteries. This development marked a significant leap forward in energy storage technology, with subsequent research leading to the exploration of various cathode materials, enhancing the safety and applications of Li-ion batteries.

The 1990s and early 2000s saw the widespread adoption of Li-ion batteries in consumer electronics, driven by their compact size, high energy density, and lightweight nature. Sony's commercialization of the first Li-ion battery in 1991 spurred a surge in applications for portable devices such as laptops, mobile phones, and digital cameras. This era of consumer electronics fueled further research and investment in battery technology, resulting in continuous improvements in performance, safety features, and cost-effectiveness.

Li-ion batteries have become the linchpin in the transformative shift towards sustainable transportation, not only powering electric vehicles (EVs) but also extending their influence to the aviation sector, drones, and aircraft. In the realm of EVs, these batteries contribute significantly to increased driving ranges, faster charging times, and improved overall efficiency. As electric mobility gains momentum, Li-ion batteries play a crucial role in reducing reliance on traditional fossil fuels, fostering a cleaner and greener transportation landscape.

Beyond land-based transportation, Li-ion batteries have found applications in the aviation industry, powering electric aircraft and contributing to the development of cleaner and more efficient aerial transportation. Electric aircraft and drones benefit from the lightweight design and high energy density of Li-ion batteries, allowing them to achieve longer flight durations, improved maneuverability, and reduced environmental impact compared to traditional combustion engines. As technological advancements continue to shape the future of transportation, Li-ion batteries stand as a versatile and indispensable solution across various modes of mobility, steering the course towards a more sustainable and environmentally conscious future.

Moreover, Li-ion batteries play a pivotal role in addressing energy challenges associated with renewable sources. As vital components of grid energy storage, these batteries enable the effective utilization of electricity generated from intermittent sources like solar and wind power. Their grid stabilization capabilities enhance the reliability of renewable energy, fostering a more resilient and sustainable power infrastructure. The applications of Li-ion batteries, spanning from personal electronics to electric vehicles and renewable energy integration, underscore their pivotal role in shaping the trajectory of technological innovation and environmental sustainability.

Li-ion batteries have become instrumental in powering space exploration endeavors, playing a critical role in sustaining the functionality of various spacecrafts and satellites. The unique properties of Li-ion batteries, such as high energy density and a lightweight design, make them well-suited for the demanding conditions of outer space. These batteries are employed in satellite systems, providing reliable and efficient energy storage for communication, navigation, and scientific instruments. Li-ion batteries are used for powering electric propulsion systems on spacecraft, contributing to efficient and precise orbital maneuvers. As the space industry continues to advance, Li-ion batteries stand as indispensable components, enabling extended mission durations and powering the cutting-edge technologies that drive our exploration of the cosmos.

Ongoing research and development initiatives continue to shape the trajectory of Li-ion battery technology. Focus areas include increasing energy density, extending cycle life, improving safety features, and addressing concerns related to raw material availability. Beyond lithium-ion, emerging technologies such as solid-state batteries and lithium-sulfur batteries are being explored for their potential to offer even higher performance and sustainability. As Li-ion batteries remain integral to various sectors, their evolutionary journey reflects the transformative impact of energy storage on our modern world.

Lithium-ion battery safety and reliability

Li-ion batteries, ubiquitous in modern technology, face significant challenges concerning safety and reliability. Among the most concerning issues is the risk of thermal runaway, where the battery can dangerously overheat, potentially leading to fires or explosions. This hazard can be triggered by various factors such as overcharging, physical damage, or flaws in manufacturing. The rapid propagation of thermal runaway throughout battery packs poses substantial risks,

particularly in high-energy-density applications like electric vehicles and large-scale energy storage systems.

Another critical concern with Li-ion batteries is the formation of dendrites, tiny lithium metal filaments that can develop within the battery. These dendrites have the potential to cause internal short circuits, compromising the battery's integrity and safety. Factors such as repeated charging cycles, high charging rates, and elevated temperatures exacerbate dendrite growth. Despite ongoing efforts to mitigate this issue through advancements in battery chemistry and manufacturing techniques, dendrite formation remains a persistent challenge in ensuring the safety and reliability of Li-ion batteries.

Moreover, the Li-ion battery supply chain presents its own set of challenges that can affect safety and reliability. The extraction and processing of raw materials like lithium, cobalt, and nickel—essential components of these batteries—can have significant environmental and social implications. Concerns such as child labor, unsafe working conditions, and environmental degradation have been raised in regions where these materials are sourced. Ensuring a responsible and sustainable supply chain is crucial not only for ethical reasons but also for maintaining the safety and reliability of Li-ion batteries.

Lithium-ion batteries and the environment

Li-ion batteries have brought significant environmental benefits across various industries. Firstly, Li-ion batteries play a crucial role in facilitating the transition to renewable energy sources by enabling efficient energy storage solutions. By storing excess energy generated from renewable sources like solar and wind power, Li-ion batteries help mitigate the intermittency issues inherent in these energy systems, thus supporting the integration of more clean and sustainable energy

into the grid. This reduces reliance on fossil fuels for electricity generation, leading to lower greenhouse gas emissions and contributing to efforts to combat climate change.

Secondly, the use of Li-ion batteries in electric vehicles (EVs) has substantial environmental advantages. EVs powered by Li-ion batteries produce zero tailpipe emissions, significantly reducing air pollution in urban areas and improving air quality. Furthermore, when coupled with renewable energy sources for charging, EVs offer a truly green transportation solution, minimizing the environmental footprint associated with conventional gasoline-powered vehicles. Additionally, the recyclability of Li-ion battery further enhances their environmental credentials, as materials recovered from spent batteries can be reused in new battery production, reducing the demand for virgin resources and minimizing waste generation.

On the other hand, the use of Li-ion battery also brings environmental concerns. One major issue is the extraction and processing of raw materials required for Li-ion battery, such as lithium, cobalt, and nickel. Mining activities for these materials can lead to habitat destruction, deforestation, and pollution of air, water, and soil. This also promotes the exploitation of impoverished locals in countries which hold the metal reserves for the lithium-ion battery manufacturing as seen in the Democratic Republic of Congo. Additionally, the disposal of Li-ion battery poses challenges, as they contain toxic chemicals and heavy metals that can leach into the environment if not properly managed. Improper disposal methods, such as landfilling or incineration, can result in environmental contamination and harm ecosystems. Furthermore, the energy-intensive manufacturing process of Li-ion batteries contributes to greenhouse gas emissions, exacerbating climate change. Efforts to address these environmental concerns include improving recycling infrastructure, promoting sustainable sourcing of raw materials, and developing alternative battery chemistries with lower environmental footprints.

Second life use

Repurposing

Used Li-ion batteries, while no longer suitable for their original applications due to decreased capacity or performance, still retains a significant amount of energy storage capability. Repurposing these batteries for a second life use offers a sustainable solution to extend their useful lifespan and reduce environmental impact. One common approach is to utilize retired Li-ion battery for stationary energy storage applications, such as grid-scale energy storage systems or home energy storage units. These batteries, when aggregated into large-scale energy storage installations, can help balance supply and demand on the electrical grid, store excess renewable energy for later use, and provide backup power during grid outages. By giving used Li-ion batteries a second life in stationary energy storage, we can maximize their value and minimize waste while promoting the transition to renewable energy sources.

Furthermore, used Li-ion batteries can be repurposed for mobile applications, such as powering electric bicycles, scooters, or small-scale electric vehicles. While these applications may not require the same level of performance as new batteries, repurposed batteries can still provide sufficient energy storage capacity for short-distance commuting or recreational use. Retrofitting used batteries into electric bicycles or scooters offers a cost-effective and sustainable alternative to purchasing new batteries, extending the lifespan of these batteries and reducing the demand for new materials. Additionally, repurposing used Li-ion batteries for small-scale electric vehicles can help reduce greenhouse gas emissions from conventional transportation and promote sustainable mobility solutions in urban areas.

Recycling

The recycling process typically involves collection, sorting, and mechanical separation, followed by chemical processing to extract key materials such as lithium, cobalt, nickel, and manganese. These recovered materials can then be purified and reused in the production of new batteries, reducing the demand for virgin raw materials and the associated environmental footprint of mining. Additionally, recycling helps prevent hazardous materials from entering landfills, where they could pose significant environmental and health risks. Recycling techniques for Li-ion batteries can be broadly categorized into three main approaches: pyrometallurgical, hydrometallurgical, and direct recycling.

1. Pyrometallurgical Recycling:

   This method involves high-temperature processing, where batteries are smelted in a furnace to recover valuable metals. The process can efficiently extract cobalt, nickel, and copper by melting them into an alloy while separating other materials as slag.

2. Hydrometallurgical Recycling:

   This technique uses chemical leaching to dissolve and separate metals from the battery materials. Typically, acids or other solvents are used to extract lithium, cobalt, nickel, and manganese from the shredded battery materials.

3. Direct Recycling:

   Direct recycling aims to recover and reuse entire components of the battery, such as the cathode and anode materials, without breaking them down into their elemental forms.

Lithium-ion battery testing

The thorough testing of Li-ion batteries is integral to ensuring their safety, reliability, and efficiency across diverse applications. From handheld electronics to electric vehicles and large-

scale energy storage systems, rigorous testing protocols are vital for validating battery performance, mitigating potential safety hazards, and refining battery designs. These testing procedures encompass a broad spectrum of assessments, including electrical, mechanical, and thermal evaluations, as well as examinations of durability, lifespan, and environmental impact. Through extensive testing, researchers, manufacturers, and regulatory bodies aim to advance battery technology, tackle emerging challenges, and fulfill the increasing demand for effective and sustainable energy storage solutions.

Electrical Performance testing

Testing the electrical performance of Li-ion batteries involves a comprehensive evaluation of their behavior under different operating conditions. These assessments are fundamental for understanding how batteries respond to charging and discharging, determining their capacity, assessing internal resistance, and gauging overall efficiency. Various tests are conducted to achieve these objectives:

1. Coulombic efficiency measurement:

   Coulombic efficiency measures the actual charge stored during discharge relative to the theoretical charge expected based on the applied current. This metric helps to evaluate the battery's efficiency in storing and releasing electrical energy, pinpointing any inefficiencies or losses during charge and discharge processes.

2. Internal resistance measurement:

   Internal resistance testing involves determining the resistance within the battery cell, impacting its voltage drop during charge and discharge. By analyzing the voltage drop across the battery terminals under diverse load conditions, this test reveals crucial information about the battery's performance, efficiency, and power delivery capabilities.

3. Life cycle testing:

   Li-ion battery life cycle testing is a systematic evaluation process aimed at understanding the performance and longevity of these batteries. Conducted under controlled laboratory conditions, the testing involves subjecting the batteries to repeated cycles of charging and discharging while monitoring various performance metrics such as capacity retention, internal resistance, and voltage characteristics. The number of cycles completed by the battery is meticulously recorded, so that its degradation over time can be tracked. Any premature failures are analyzed to identify root causes and improve future designs. The testing continues until the battery reaches its end-of-life criteria, at which point data analysis provides insights into the battery's overall performance and durability. This information is crucial for refining battery designs, enhancing manufacturing processes, and optimizing usage recommendations for different applications, ensuring the reliability and safety of Li-ion batteries in consumer electronics, electric vehicles, and energy storage systems.

Abuse Testing

Li-ion battery abuse tests are designed to simulate extreme conditions and abusive scenarios that batteries might encounter during transportation, handling, or usage. These tests aim to evaluate the battery's safety features and resilience to abuse, such as overcharging, short circuits, physical damage, and exposure to high temperatures.

1. Short circuit testing:

   Short circuit testing of Li-ion batteries is a critical safety evaluation procedure aimed at understanding the response of batteries to extreme conditions. By intentionally creating an electrical connection between the positive and negative terminals, simulating an

unintended short circuit scenario, researchers can assess the battery's reaction, including temperature changes, gas emissions, and potential hazards such as fire or explosion. This testing provides valuable insights into the effectiveness of safety features and mechanisms within the battery, guiding the development of safer battery designs and enhancing safety protocols for various applications, from portable electronics to electric vehicles and grid-scale energy storage systems.

2. Overcharge/discharge testing.

   Overcharge and over discharge testing of Li-ion battery is fundamental to evaluating their safety and performance characteristics. During overcharge testing, batteries are intentionally charged beyond their recommended voltage limits to simulate scenarios where charging control mechanisms fail or are overridden. This process assesses the battery's ability to withstand overcharging without catastrophic failure, such as thermal runaway or venting. Similarly, over discharge testing involves discharging batteries beyond their minimum voltage thresholds, mimicking situations where devices continue to draw power even after the battery is depleted. This evaluates the battery's resilience to over discharge-induced damage, including capacity degradation or irreversible chemical changes.

3. Crush testing:

   Lithium-ion battery crush testing is a vital safety evaluation process that simulates scenarios where batteries experience mechanical stress, such as in accidents or mishandling. During crush testing, batteries are subjected to controlled pressure from hydraulic or mechanical presses, mimicking conditions where batteries are compressed or crushed.

Other types of abuse testing include puncture testing, bend testing, drop testing and vibration testing etc.

Thermal and Environmental testing

Thermal testing of Li-ion battery involves evaluating their behavior and performance under different temperature and environmental conditions. Some of these tests are listed below:

1. Water Ingression:

   Water ingression testing in Li-ion battery is a critical evaluation procedure aimed at assessing the battery's resistance to water exposure and its potential impact on performance and safety. During this testing, batteries are subjected to controlled levels of water ingress through various means, such as immersion or spray testing, to simulate real-world scenarios where batteries might come into contact with water due to accidents or environmental conditions.

2. Thermal runaway testing

   Thermal runaway testing is a crucial safety assessment method employed to evaluate the response of Li-ion batteries to extreme temperature conditions. During this testing, batteries are subjected to controlled temperature increases beyond their operational limits, simulating scenarios where heat buildup occurs due to external factors like overcharging, short circuits, or exposure to high temperatures. The objective is to observe the battery's behavior under such conditions, including the potential for self-heating, gas generation, and violent reactions leading to thermal runaway—a catastrophic chain reaction characterized by rapid heat release and battery failure.

3. High/Low temperature storage and performance testing:

High and low-temperature storage and performance testing of batteries are essential procedures aimed at evaluating battery behavior and performance under extreme temperature conditions. High-temperature storage testing involves subjecting batteries to elevated temperatures, typically above 60°C, to simulate environments such as hot climates or the interior of electronic devices during operation. Conversely, low-temperature storage testing exposes batteries to sub-zero temperatures, often below -20°C, to replicate cold weather conditions or storage in unheated environments.

Besides these tests thermal cycling, salt spray test, heat generation measurement, humidity test and altitude tests are also conducted to understand the dependence of Li-ion batteries on their environment.

Lithium-ion battery internal resistance

Internal resistance measurement is integral to this research as a lot of battery behavior can be explained in terms of its internal resistance. By measuring the internal resistance of the battery, its SOC, SOH, ESC behaviors and ageing etc. can be assessed in Li-ion batteries has been studied through different methods and technologies as it is a critical aspect of assessing their performance and health. Its dependent on many factors such as:

Dependencies

1. Temperature

   Temperature can be the biggest foe to the performance of Li-ion batteries. While high temperature causes a battery to heat up at unprecedent rates by slowing down the dissipation of heat from a charging or discharging battery and leading to thermal runaway. Lower temperatures affect the performance of Li-ion batteries, and it can be quantified by an increase in internal resistance [1]. Lower than normal environmental

temperature can cause the solidification of electrolyte, dendrite formation on anode, uptick in polarization processes and thus increasing the resistance to the flow of charge through the battery. This causes the internal diffusion to reduce which in turn increases the charge transfer resistance [2]. Besides this, contact resistance between separator and both electrodes affects thermal resistance which in turn impacts its internal resistance [3]. Batteries should be operated between the temperature range provided by the manufacturers.

2. State of Health

   According to [4][5][27], magnitude of discharge current and state of health also affect the internal battery resistance. Battery state of health changes over its lifetime. It is used to quantify the useful life left in a battery. As a battery ages, the charge that a battery can accept in a fixed amount of time decreases due to the increase in its internal resistance and it can be measured by the heat dissipation in ana ageing battery.

3. State of Charge

   The state of charge (SOC) of Li-ion batteries is intricately linked to their internal resistance. As the SOC decreases, particularly when the battery approaches a fully discharged state, the internal resistance typically increases. This rise in internal resistance at low SOC levels can lead to greater heat generation and reduced efficiency during discharge, this means that the battery's usable capacity will be reduced [28]. Conversely, when the battery is near full charge, the internal resistance is generally lower, allowing for more efficient energy transfer. This relationship is critical for optimizing battery performance, as managing SOC within an optimal range helps maintain lower internal resistance, enhancing the overall efficiency, lifespan, and safety of Li-ion batteries.

4. Battery Chemistry

   Battery chemistry, environmental conditions, and operating conditions are responsible for ageing batteries which leads to changes in internal resistance [6]. The chemistry of Li-ion batteries significantly influences their internal resistance, impacting overall performance and efficiency. Different cathode materials (such as lithium cobalt oxide, lithium iron phosphate, and lithium nickel manganese cobalt oxide) and anode materials (such as graphite and silicon) exhibit varying levels of conductivity and ionic mobility, which directly affect the internal resistance. For instance, lithium iron phosphate (LiFePO4) batteries tend to have higher internal resistance compared to lithium cobalt oxide (LiCoO2) batteries, due to differences in ion mobility and electrical conductivity. Additionally, the electrolyte composition and the presence of solid electrolyte interphase (SEI) layers also play crucial roles in determining internal resistance. Optimizing the chemistry of Li-ion batteries, therefore, is essential for minimizing internal resistance, which in turn enhances charge/discharge rates, energy efficiency, and battery lifespan.

Measurement

The impedance measurement provides information about the internal resistance of the battery, which is a combination of several factors including the resistance of the electrolyte, electrodes, and internal connections. This resistance can change over time due to factors such as aging, temperature, and cycling. By analyzing the internal resistance measurements over time, researchers can monitor the health of the battery and identify any degradation or anomalies that may indicate potential issues.

The 2 RC (two resistor-capacitor) equivalent circuit model is widely used to simulate the dynamic behavior of Li-ion batteries, capturing both the transient and steady-state characteristics

of the battery’s response to load changes. This model comprises an open-circuit voltage (OCV) source representing the battery’s equilibrium voltage at a given state of charge (SOC), a series resistance Ro accounting for instantaneous voltage drops due to internal resistance, and two parallel RC networks to represent the electrochemical dynamics. The first RC network, consisting of R1 and C1, typically models the short-term, high-frequency response related to the charge transfer resistance and double-layer capacitance at the electrode/electrolyte interface. The second RC network, with R2 and C2, captures the slower, low-frequency processes such as diffusion of lithium ions within the electrode materials. By fitting experimental pulse discharge data to this model, the parameters Ro, R1, R2, C1 and C2 can be extracted, enabling accurate simulation of the battery's voltage response under various operating conditions, which is crucial for battery management systems in optimizing performance and longevity.

1. Ohmic resistance

   Ohmic resistance in Li-ion batteries, often referred to as series resistance or R0R_0R0, represents the immediate voltage drop when a current is applied, encompassing the resistance of the electrolyte, electrodes, and interconnections within the cell. This resistance is primarily influenced by the materials used in the battery and the quality of the electrical contacts. High ohmic resistance leads to significant energy losses as heat, reducing the efficiency of the battery, especially at high discharge rates. It also causes an immediate voltage drop upon load application, which can impact the performance of the battery in applications requiring high power. Minimizing ohmic resistance through the use of highly conductive materials and improved cell design is essential for enhancing the overall performance and efficiency of Li-ion battery.

2. Polarization resistance

Polarization resistance, on the other hand, includes the resistive elements associated with electrochemical processes within the battery, divided into charge transfer resistance and diffusion resistance. Charge transfer resistance is related to the kinetics of the electrochemical reactions at the electrode/electrolyte interface, which can vary with the state of charge, temperature, and the specific materials used in the electrodes. Diffusion resistance, also known as Warburg impedance, is associated with the transport of lithium ions through the electrolyte and into the active material of the electrodes. Both components contribute to the time-dependent voltage drop observed during battery operation. High polarization resistance can limit the rate at which the battery can be charged or discharged, affecting the overall power capability and efficiency. Understanding and optimizing polarization resistance is crucial for improving the performance and lifespan of Li-ion battery, making it a key focus area in battery research and development.

Pulse Discharge Testing

Pulse discharge testing is a vital method for assessing the performance and dynamic characteristics of Li-ion batteries. This test involves subjecting the battery to short bursts of high current, followed by rest periods, to mimic real-world usage scenarios. This approach helps analyze the battery’s capability to handle rapid load changes and provides insights into its internal resistance, capacity, and efficiency. The voltage response to the current pulses allows for the extraction of equivalent circuit parameters, such as series resistance and RC time constants, which are essential for modeling the battery's behavior. Pulse discharge testing also reveals information about the battery’s thermal performance and the effects of high-current loads on degradation mechanisms. By capturing these transient responses, engineers can optimize battery

design and management systems, ensuring improved performance and longer lifespan in practical applications.

Figure 2 illustrates 10 equally wide pulses of current applied at constant intervals. The voltage recorded in response to these current pulses is used to extract values of Ro, Rp (R1, R2), C1, and C2, as shown in Figures 1 and 3. The immediate and instantaneous voltage drop at the beginning is due to Ro, while the gradual decrease in voltage is attributed to the polarization reactions occurring within the battery.

The internal resistance measurement is interpreted in conjunction with other battery performance metrics such as capacity, voltage, and cycle life. An increase in internal resistance over time may indicate degradation or damage to the battery, while a sudden change could be a sign of an internal fault or manufacturing defect. Understanding these trends helps in diagnosing battery health and optimizing battery management strategies.

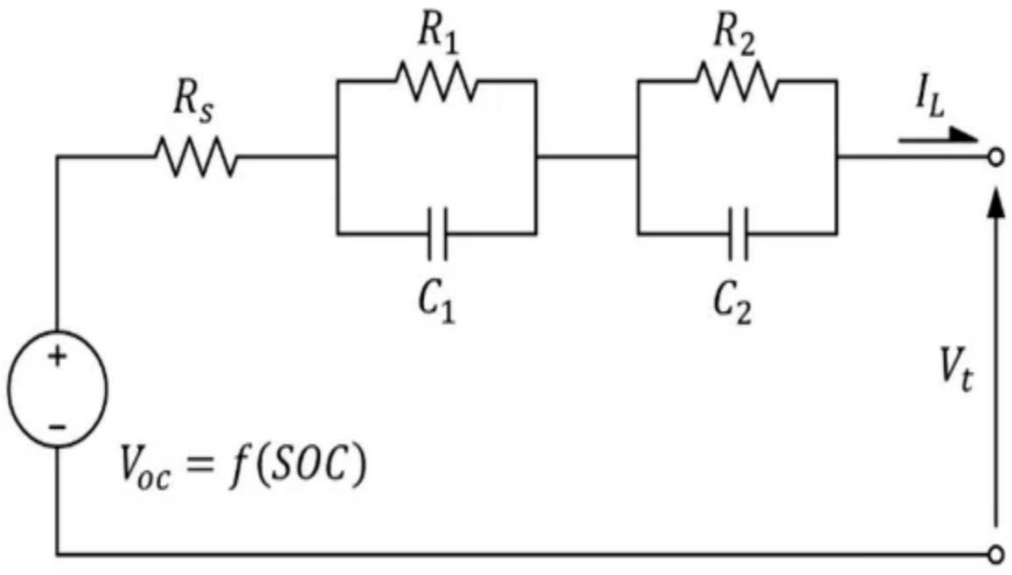

Figure 1. 2RC Equivalent Circuit

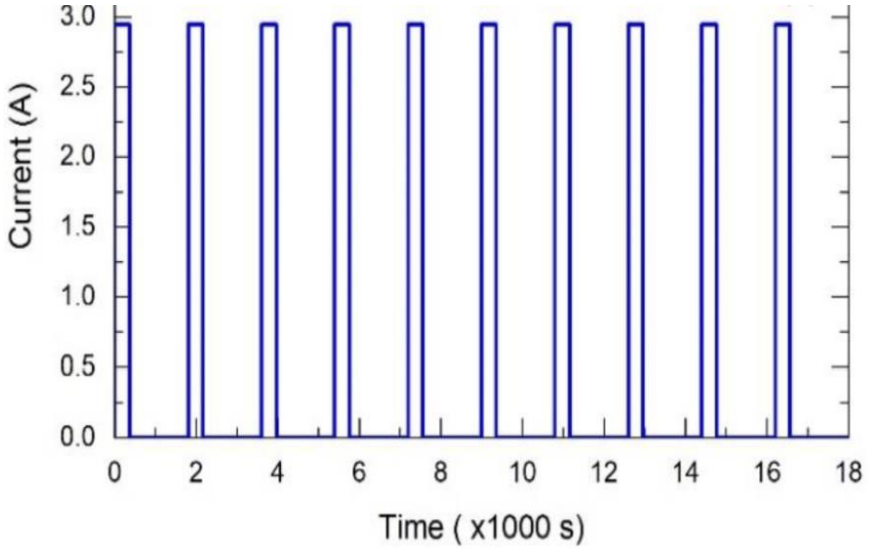

Figure 2. Current pulses for PDT

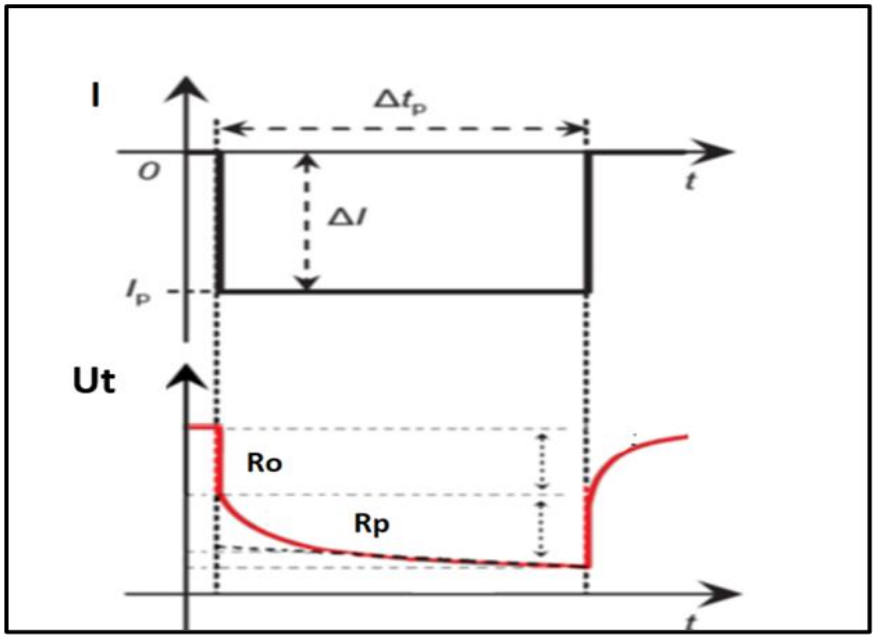

Figure 3. Parameter extraction from PDT

Problem Statement

It is noteworthy that contemporary research into short circuits and thermal runaway primarily focuses on internal short circuits (ISC), despite a significant number of battery-related fires being

caused by external short circuits (ESC). Understanding internal battery parameters during an ESC is crucial, yet there is limited data available to analyze these trends and dependencies. Short circuit tests (SCTs) are designed to provide insights into the battery's response during a short circuit event as well as its behavior afterward. This means that a battery may not experience enough damage during an ESC to render it useless, potentially avoiding the need for immediate disposal—a point that even the most comprehensive studies often overlook. Consequently, a post-external short circuit battery (PESCB) that has recently undergone an ESC might still be usable, rather than ending up in a landfill.

Plan of Action

Battery abuse and short circuit tests require sophisticated and costly equipment, including battery cyclers, thermal chambers, containment facilities, and programmable loads. These tests also entail significant safety risks due to the high currents involved, rising temperatures, and the inherently volatile nature of batteries. For instance, the external resistance used in External Short Circuit Tests (ESCT) is set at 5 milliohms according to IEC62660-2 [11], underscoring the critical importance of safety measures. Personnel conducting these tests must be thoroughly trained in electrical safety protocols and hazard mitigation.

During an ESC, battery current spikes initially and then gradually decreases until the battery is fully discharged. This behavior can be described as a piece-wise function, where the current in the first region (the initial spike), the second region, and the third region depends on the total ohmic resistance, mass transport within the battery, and the diffusion of lithium ions through the battery separator, respectively [12-14]. Detecting and assessing the severity of a short circuit promptly in the first region is crucial, as it can prevent a soft short circuit from escalating into a hard short circuit [15]. Additionally, if controlled, this process can be used to warm up batteries

in extremely cold weather [16]. The current spike occurs within the first second of ESC initiation [17][18] and is influenced by the cell's ohmic resistance (Ro) [19].

Executing ESCTs involves using battery cyclers, control and automation hardware, thermal chambers, and other expensive equipment. High-quality data collection, reflecting the true ESCT from initiation to conclusion, is vital. To reduce costs, many ESCT setups use relays or other mechanical switches as cost-effective alternatives to battery cyclers [13][20]. For example, a relay is used for switching during a long-duration ESCT on Nickel Cobalt Aluminum (NCA) and Nickel Cobalt Manganese (NCM) Li-ion batteries as shown in figure 4[14]. However, mechanical switching can introduce unwanted pulsating spikes or bouncing in the recorded data, unrelated to the short circuit. This bouncing, occurring between 0.002s and 0.02s, can lead to misleading values of maximum current, ohmic resistance, and total internal resistance of the battery. Accurate internal resistance measurement is crucial for preventing and controlling DC arcs, efficient BMS design [21], and voltage sag analysis.

To assess electrochemical changes in the battery, pulse discharge tests (PDTs) followed by internal parameter estimation are conducted. In MPDT [15], the battery is discharged in short pulses at multiple C-rates with rest periods. The current and voltage data from MPDT are used to extract parameters for equivalent battery circuits, defining the battery's electrochemical behavior in terms of passive circuit components like ohmic and polarization resistances.

After a short circuit, a battery can be potentially damaged, often leading to quick disposal. However, smart battery management systems, protective circuitry, and controlled short circuits can interrupt a short circuit before it causes irreversible damage [22]. Post-short circuit, the battery might not be suitable for its original application but could still be useful in less demanding applications, depending on the extent of the damage, environmental temperature, and

short circuit duration. For example, batteries with 70-80% performance are unsuitable for electric vehicles but can be used in consumer electronics [23]. Similarly, a battery might be usable after a brief ESCT from a capacity fade standpoint [15], but changes in internal resistance across different SOCs can limit its usability under certain conditions.

A Li-ion battery's capacity and internal resistance are crucial for identifying its SOH. These factors, however, are not directly proportional. Internal resistance depends on various factors, notably SOC. During aging, events like lithium plating on electrodes, particle cracking, and collector corrosion [24] cause capacity to decrease and internal resistance to increase, but at different rates. After a short circuit, a battery's capacity reduces, and its resistance increases differently across the SOC spectrum. This means a PESCB will perform better at certain SOC points, which change as the battery ages. This information is vital for maximizing battery use before recycling or disposal.

This research's contributions are twofold. The first is an economical, zero-bounce test setup for conducting ESCTs on Li-ion batteries, effectively eliminating bouncing and spikes from data recorded at a 500µsec sampling rate. The setup's effectiveness is demonstrated through ESCTs on 21700 batteries at 25°C. It includes power MOSFETs for fast switching and low turn-on resistance [14], a real-time data acquisition (DAQ) system with a fast-sampling rate, non-inductive resistors, and an automated LabVIEW testing environment. Equivalent circuit parameters are calculated in Python using curve fitting. For each SOC point (90%-10%), a HB is retired after ESCT. Additionally, MPDT is conducted at safe discharge current levels up to 7C across different SOCs at 25°C using the same setup. Battery internal parameters from MPDT and ESCT are compared to see if ESCT discharge resembles safe current level discharge.

The second contribution is measuring the change in total internal resistance of a PESCB at different SOCs to find SOC points where the battery performs best, i.e., exhibits the least resistance. To visualize the battery's lifetime stage after a short circuit, a HB is cyclically aged, and the internal resistance of the PESCB and HB is compared at different SOCs for two ESC durations (10 and 20s). Few studies address the re-use of Li-ion batteries post-ESC based on moderate internal resistance change.

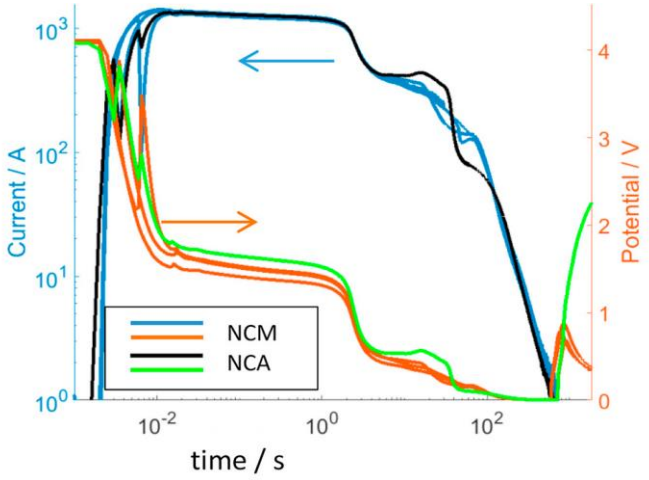

Figure 4. Bouncing during short circuit testing [14]

.

Chapter 2: Test setup design and methodology

Battery abuse and short circuit tests require sophisticated and costly equipment, involving significant safety risks due to high currents, rising temperatures, and the volatile nature of batteries. Research has shown that understanding battery behavior during an External Short Circuit Test (ESCT) is crucial, as initial current spikes followed by gradual decreases provide insights into battery performance and safety. Detecting short circuits early can prevent severe damage, allowing batteries to be repurposed rather than discarded. Cost-effective setups using relays can introduce data inaccuracies, highlighting the need for precise equipment. After a short circuit, smart management systems can prevent irreversible damage, enabling batteries to be used in less demanding applications. Capacity and internal resistance are key to identifying a battery's state of health (SOH), with their relationship influenced by various factors including SOC. This study presents an economical, zero-bounce ESCT setup and measures changes in internal resistance to optimize battery use before recycling, emphasizing the potential for repurposing batteries post-ESC based on moderate internal resistance changes. There are two parts of this problem. Part 1, which focuses on ESC and Part 2 which focuses on life cycle testing.

For part 1, MPDT has to be conducted at the following discharge rates:

1. 1.25C (5A)
2. 2.5C (10A)
3. 3.75C (15A)
4. 5C (20A)
5. 6.25C (25A)
6. 7.5C (30A)
7. 30C (120A).

Where 30C is the short circuit current and 1C-6C are safe current level discharges for the battery currently used, Samsung 21700 40T. This is a 4000mAh battery with the highest discharge current rating of 35 Amps. In MPDT, the battery is discharged in short, current durations, all the while recording the current and voltage across the battery. MPDT requires a smooth switching circuit is designed with a very high sampling rate so that the events of the beginning of discharges can be recorded. Especially in the event of an ESC, where it's of paramount importance to both detect an ESC as well as study its behavior that can later be used to design circuit protection and efficient battery management systems. This requires the right equipment that can switch without any mechanical movements such as MOSFETS and a high-speed automated control and data collection mechanism. This all was achieved by using affordable equipment, which was one of the points mentioned in the problem statement.

For part 2, a lithium-ion battery was cyclically aged. It is a HB from the same batch, make and model as of the short-circuited batteries. Cyclic ageing is a long, time taking process where the tests last months or years. These tests require that the battery is contained in a stable environment, so it is exposed to the same temperature, humidity, elevation, pressure etc throughout the duration of the test. Using a thermal chamber becomes a necessity in this kind of testing. All the battery monitoring is done from outside the thermal chamber so as to not affect the test conditions. This testing also requires a battery cycler, which can be used to conduct a multitude of tests including a cyclic ageing. This testing is also automated and done using the battery cycler tester software.

Non-Inductive resistors

Non-inductive resistors, also known as non-linear resistors, are resistors that do not exhibit inductance in their behavior. They are wire wounded resistors but on two parallel coils, such that

the direction of current flow is opposite in both coils which cancels out the resultant magnetic fields and leads to no inductance [25], whereas physical resistors have inductance or parasitic inductance. These resistors are of interest in various applications due to their unique characteristics. For instance, they are used in the validation of inductive sensors, high pulsed current measurement, and transient voltage monitoring.

For discharging the battery at different current levels, non-inductive resistors are used. The induction of a resistor becomes an important concern for high switching applications and since this testing involves fast switching, this might cause inductances to creep into the calculated parameters for short-circuit current estimation. This is another reason why any programmable loads are avoided for these tests.

Switching circuit

Bouncing in current and voltage is observed upon the circuit closure (and opening), that is, right after the short circuit initiation. The solution to this problem is to eliminate this bouncing circuit component, which is likely a mechanical switch. Therefore, a switching circuit in Fig. 2. with two parallel MOSFETs (IRFP064n) coupled with heatsinks is chosen instead, it offers fast switching and a negligible RDS(ON) (on resistance from drain to source) of 8 milliohms each. The total turn on time, t_{ON} of a MOSFET is equal to the turn on delay time and rise time whereas, the turn off time t_{OFF} is equal to turn off delay time and fall time. The t_{ON} for this MOSFET is 114ns and the t_{OFF} is 113ns. The switching is controlled by a program designed in LabVIEW.

CompactRIO

A National Instruments DAQ device, CRio, is used for data collection and controlling the MOSFET, which is responsible for turning the battery ON/OFF. CRio has access to three processors: the host computer, the real-time LabVIEW operating system processor, and the

reprogrammable FPGA. The host computer serves as a human-machine interface, while the FPGA module provides very fast hardware-based switching, sampling, triggering, and data reading capabilities. In the FPGA VI, as shown in Figure 5, the MOSFET switching is controlled. For instance, a “0” is applied to the analog output pin 0 for 6 seconds, then replaced with a “7” for another 6 seconds. The “0” at the MOSFET gate means no conduction between the drain and source, resulting in no current flow in the circuit, leaving the battery in an open circuit state. Applying a “7” across the gate switches on the MOSFET, enabling conduction between the drain and source with a negligible resistance of 8 milliohms. If the signal is less than “7”, the MOSFET switches on, but the current flow will be minimal and dissipated as excessive heat. The top half of the FPGA VI shows a while loop responsible for reading inputs from analog input pins 0 and 4 at a very fast sampling rate. This while loop operates continuously from the beginning to the end of the test, reading data simultaneously and using a build array function to combine the data into an array before storage. The FIFO (first-in, first-out) module inside the for loop is crucial to this LabVIEW logging program.

In LabVIEW, FIFO (First-In, First-Out) is a crucial data storage and buffering method used to manage data flow efficiently in applications requiring real-time processing and precise timing. FIFO structures ensure data is processed in the order received, preventing data loss and ensuring synchronization across different processes. LabVIEW leverages FIFOs for tasks like buffering data between hardware I/O operations and software processing, enabling smooth and continuous data streams even with variations in processing times. This technique is particularly useful in data acquisition, where maintaining the data sequence is critical. Additionally, LabVIEW's FIFO implementation allows for customizable buffer sizes, providing flexibility to accommodate varying data rates and ensuring systems can handle data bursts without overflow, enhancing the

robustness and reliability of real-time applications. FIFOs help decouple data producers (e.g., hardware acquisition) from data consumers (e.g., software processing), allowing independent operation at different speeds without data loss. This module handles high data throughput efficiently, making it suitable for applications involving large amounts of data, such as data acquisition systems, signal processing, and communication systems.

The actual loop rate shows the time difference between two consecutive executions of the loop to detect any possible issues or inconsistencies in data recording time, calculated by subtracting the two times. The Real-time module in CRio processes data and logs it onto the RT controller part. The RT VI, shown in Figure 6, is programmed to read data from the temporary FIFO, where the FPGA VI stores the data. An FPGA target block diagram helps connect the FIFO from the FPGA VI to the RT VI. After the FIFO is initialized, a TDMS file is created on the CRio system to hold all the recorded current, voltage, and timing data. An RT VI is connected to a while loop, which runs until the FIFO is empty. Inside the while loop, data is read from the FIFO and restructured, with recorded data affixed to proper timestamps and stored in the TDMS file on the CRio permanently unless deleted. Two TDMS write functions write the timestamps and the decoupled analog data to the TDMS file created earlier. From the CRio, this file can be transferred to a desktop computer and analyzed. The CRio is programmed in LabVIEW FPGA interface mode to achieve all of this, tapping into the full potential of CRio by tailoring the FPGA functionality alongside programming the real-time processor, achieving performance levels usually associated with bespoke hardware solutions [26]. This automated data collection and switching system has a sampling time of 500 microseconds, with differential input mode used to limit noise incorporation into the signals.

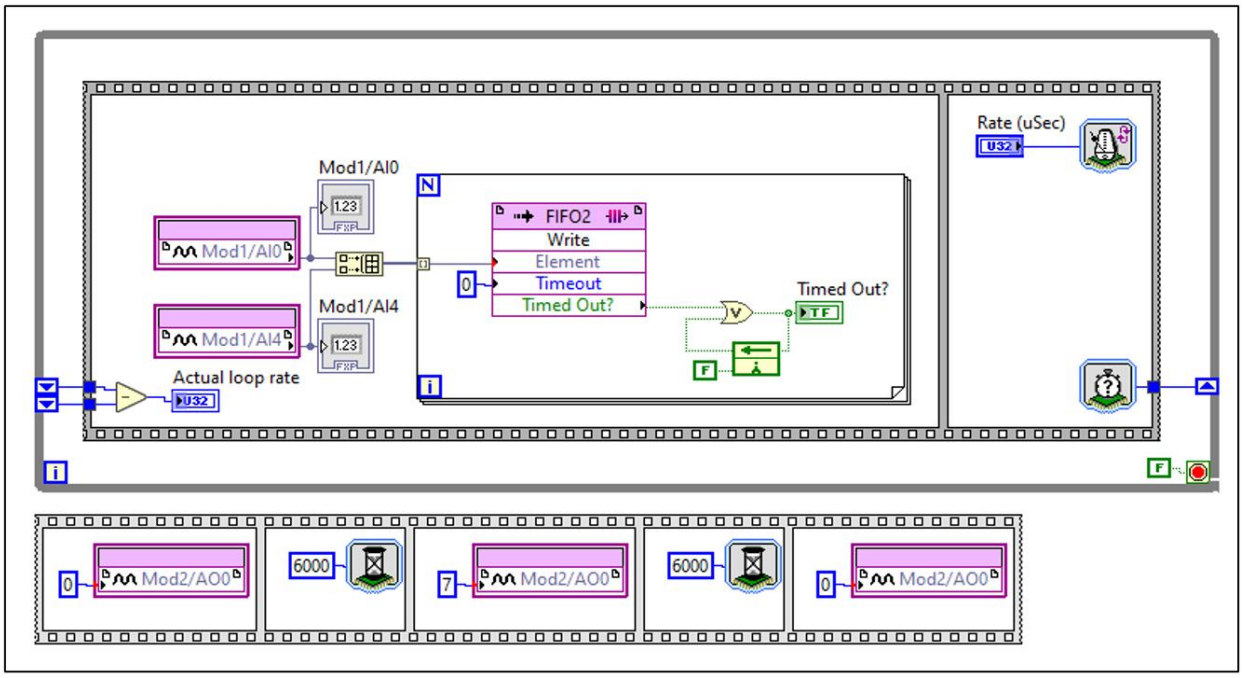

Figure 5.FPGA VI Block Diagram

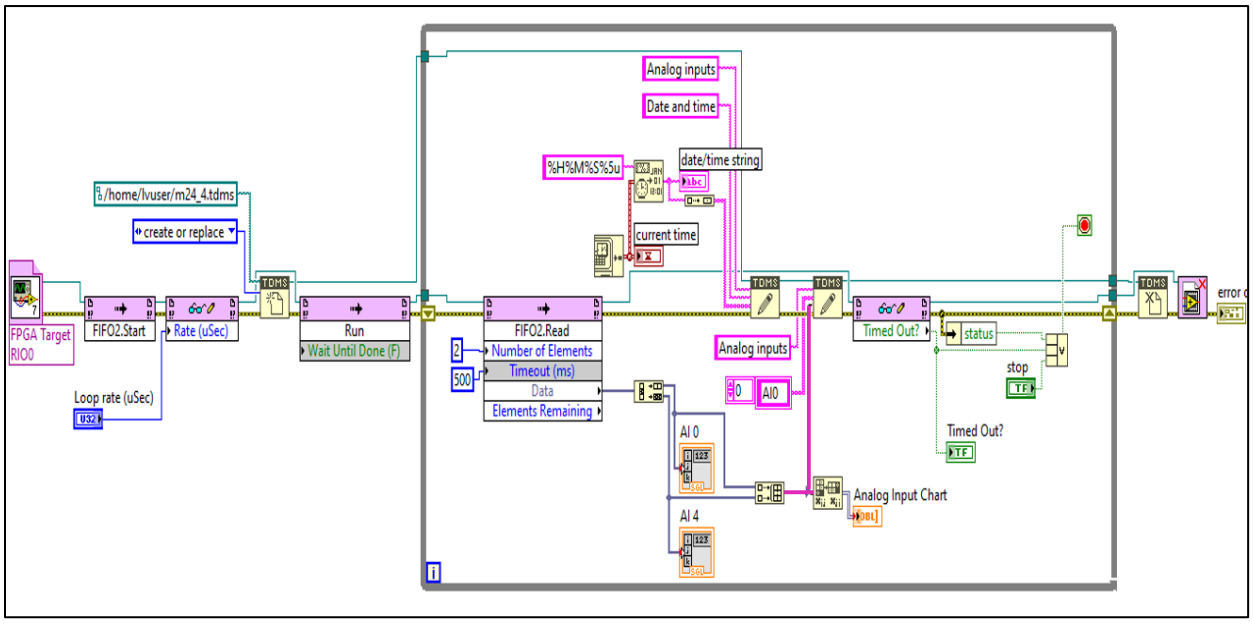

Figure 6. RT VI Block Diagram

Thermal Container

The battery is contained in a makeshift thermal chamber at 25℃. It consists of a small fridge which is capable of both heating and cooling as seen in part 1 of figure 7. The temperature of this thermal chamber is controlled by a temperature regulating device which can control both cooling or heating of this fridge based on the temperature setting on the monitor, where the top value is room temperature, and the value below is the desired temperature (part 2 of figure 7.). Part 3 shows the connection of the thermal chamber to this regulating device. If we need to control the cooling, the thermal chamber is plugged in the cooling socket and when it needs to be heated it's plugged into the socket labeled heating. The regulating device works by measuring the temperature of the inside of the thermal chamber with the help of a small thermometer attached to it which is placed inside the thermal chamber (part 4). For reference the readings from the regulating device are compared to the readings from the thermometer (part 5).

Figure 7. Makeshift thermal chamber

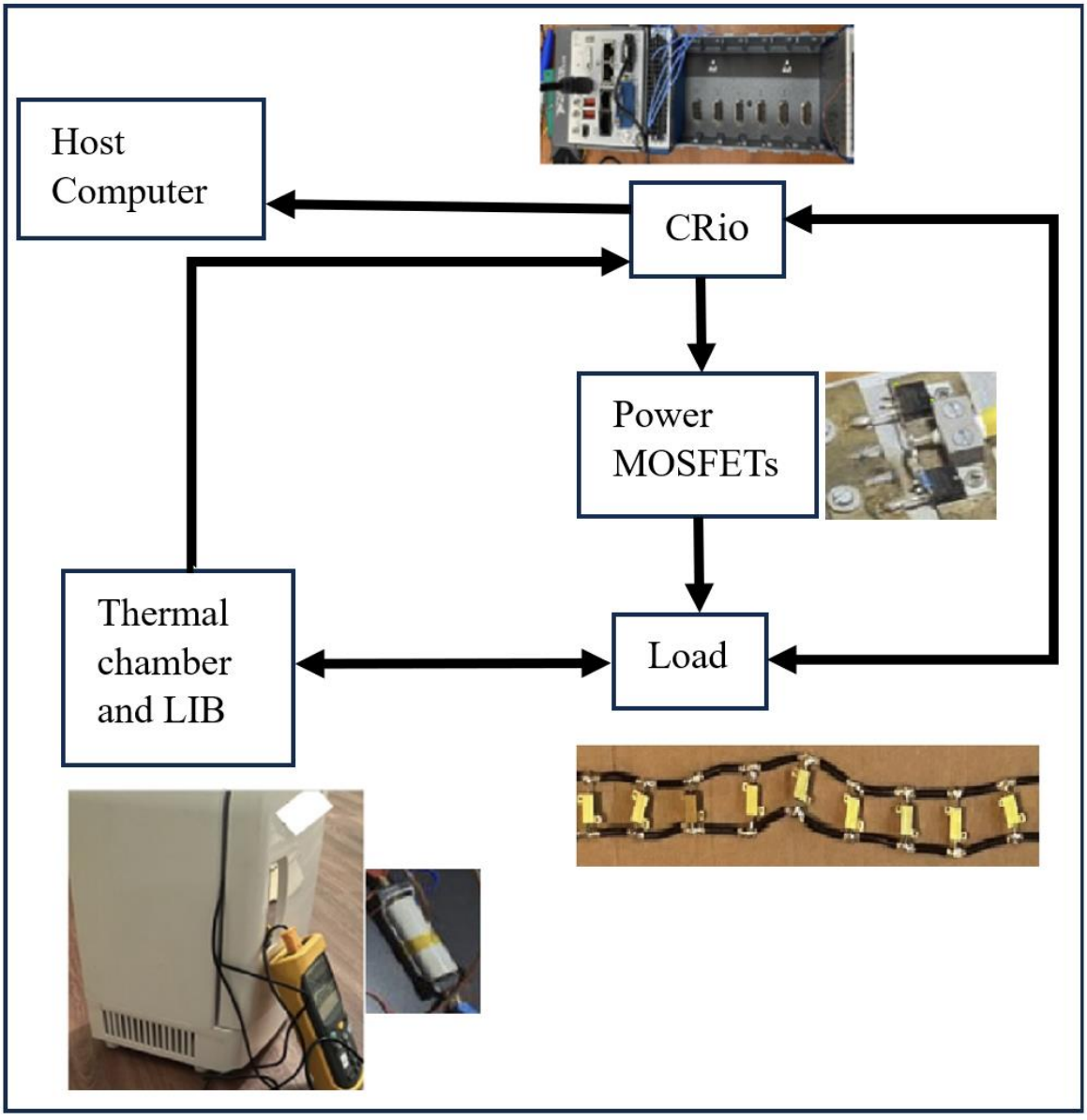

Figure 8. Testing setup

Automated Data Collection and switching

As a part of preparing the battery, a small battery management system monitors and controls the battery charging so that the battery is in its optimum state for the tests. Before the experiments, the battery is preconditioned; by discharging, charging and then leaving it to rest for 4 hours as its understood that after 4 hours a Li-ion battery reaches its stable state [30].

Using the switching circuit and the automated switching designed in LabVIEW, MPDT can be conducted. One thing that has to be decided before conducting an MPDT is the duration of the discharge pulse, that is how long will the battery remain connected to the load? [29] suggests using a pulse duration based on the application. Since the purpose of all the MPDT conducted during this research is ESCs and their effect on the Li-ion batteries, pulse duration is kept at 10s. It is kept at 10s because in modern day electronics a fault such as an ESC longer than 10s won't be a feasible choice. So protective circuitry and the BMS will detect the ESC and make attempts to put an end to it by opening the effected part of the circuit or disconnecting the entire battery from the rest of the circuit using circuit breakers, relays and fuses. Consequently, because the pulse duration for the ESC tests is kept at 10s, the reference set of MPDTs conducted for comparison purposes at 5A to 30A also have a duration of 10s. For each of the discharge rates mentioned, the battery is pulse discharged at nine SOC levels (90% - 10%). It is made sure that before conducting an MPDT that the battery is at the correct SOC state. For instance, to obtain the values of battery equivalent circuit parameters for 10A at 40% SOC, the battery should have rested and reached the 40% SOC level before its subjected to this test. Since different discharge pulse levels are used, the battery might not be at 40% after the previous discharge pulse and hence is brought to this SOC level through appropriate methods. The following test profile, in figure 9, is repeated for nine SOC levels:

1. Rest period when the battery is at open circuit state.
2. Battery is subjected to a 10 second discharge by connecting a load across it.
3. The discharge pulse is removed and the battery rests for 1 hour.
4. The battery is subjected to a discharge current that removes x% of its charge in order to reduce its SOC by 10% as compared to the beginning of the previous pulse.

5. The rest period of 30 minutes to revert the battery to its open circuit state.

One ESCT at 70% SOC was kept at 20s long, its results and reasoning will be discussed in the next sections. Since, this is a short circuit study aimed at gathering short circuit prediction data without glitches and bouncing, the sampling period is kept very small at 500µs

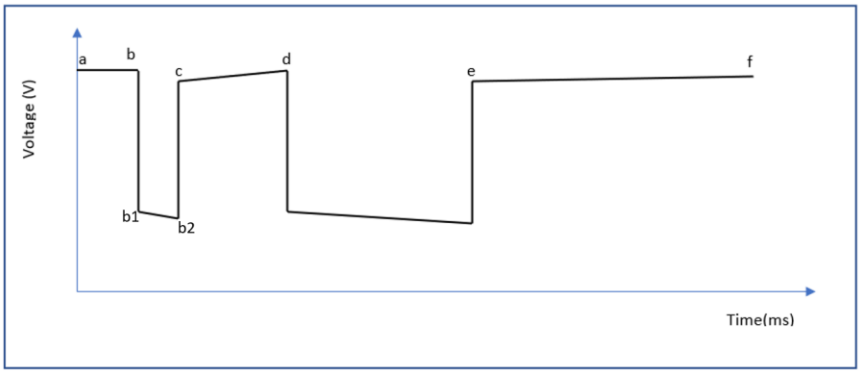

Figure 9. PDT profile

Battery cycler-thermal chamber

Part 2 of this research focuses on aging cells and building a case for their reuse after an abusive event. For battery aging tests, batteries are stored in thermal chambers and connected to a battery cycler. The thermal chamber helps maintain the ambient temperature of the battery setup at 25°C. A type K thermocouple is connected to the battery to log its surface temperature and halt the test if any hazardous situation arises. The battery cycler is programmed to charge and discharge the battery up to a given number of cycles, while staying within the lower and upper cut-off limits of current, voltage, temperature, and capacity provided at the beginning of the test.

Figure 10 shows the battery cycler software window, which can look different based on the brand of the battery cycler used. The figure shows CC_Dchg (constant current discharge) for 1s at a 1C rate, followed by CC_Dchg for 10s at a 0.1C rate. The last step shown is "Cycle," which cycles a certain step or steps a given number of times. This software also allows you to add tasks such as

constant current charge, constant voltage charge, constant current-constant voltage charge, constant power charge, constant voltage discharge, constant current-constant voltage discharge, constant power discharge, constant resistance discharge, cycle, rest, end, etc. Different values of voltage, current, and capacity can be provided for each step.

Figure 11 shows inputs coming from battery cells connected to the battery cycler. Red, black, and white cables are for voltage and current. The blue cables are for temperature readings from the thermocouple attached to the battery cells using Kapton tape.

Figure 12 shows the thermal/environmental chamber that houses the batteries. The temperature can be set from the HMI (human-machine interface) shown on the right, allowing time for the inside temperature to reach the desired level.

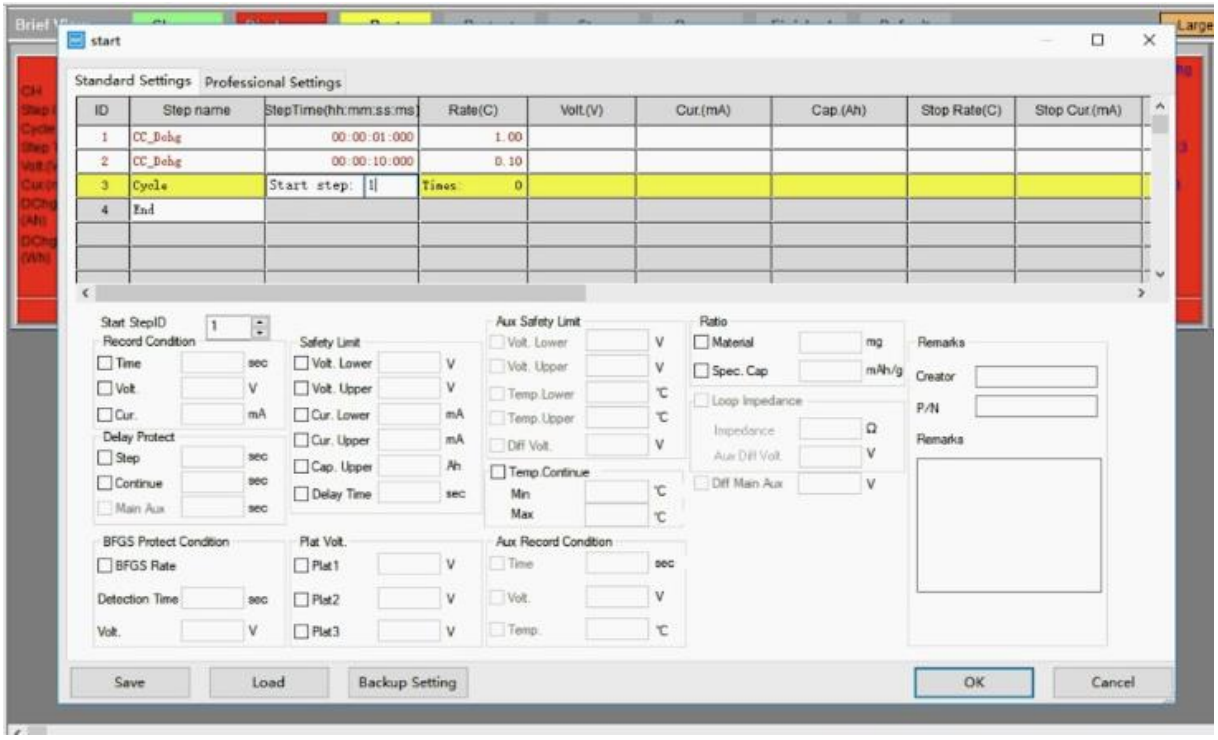

Figure 10. Battery cycler software

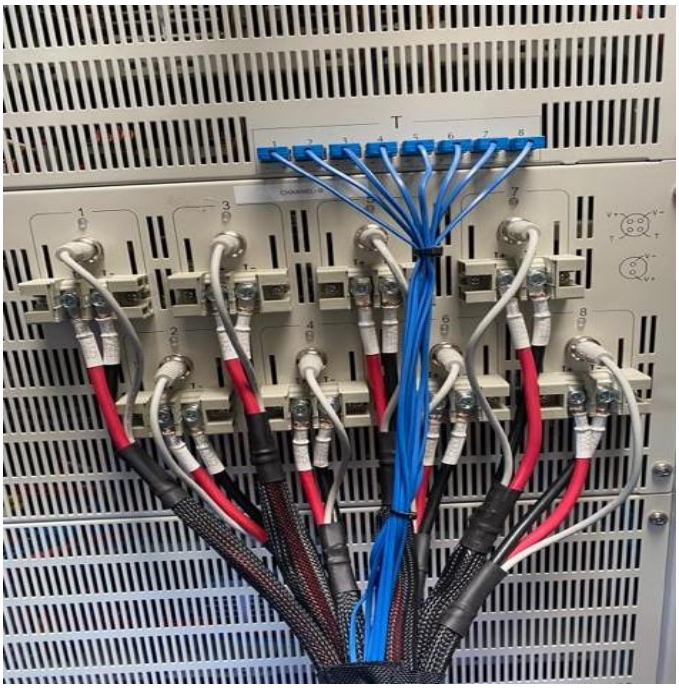

Figure 11. Battery cycler

Figure 12. Thermal chamber housing the battery cell.

Battery cycling profile used in this study is listed below and shown in figure 13:

1. Constant Current (CC)-Discharge of battery at 0.5 C
2. Rest battery for 30 minutes
3. CC-Constant Voltage (CV)-Charging of battery at 4.2 V and 0.5C
4. Rest battery for 2 hours
5. CC-Discharge battery at 1C until the lower voltage cut-off point is reached.
6. Go to step 3. Repeat n (a pre-set number of testing) times.

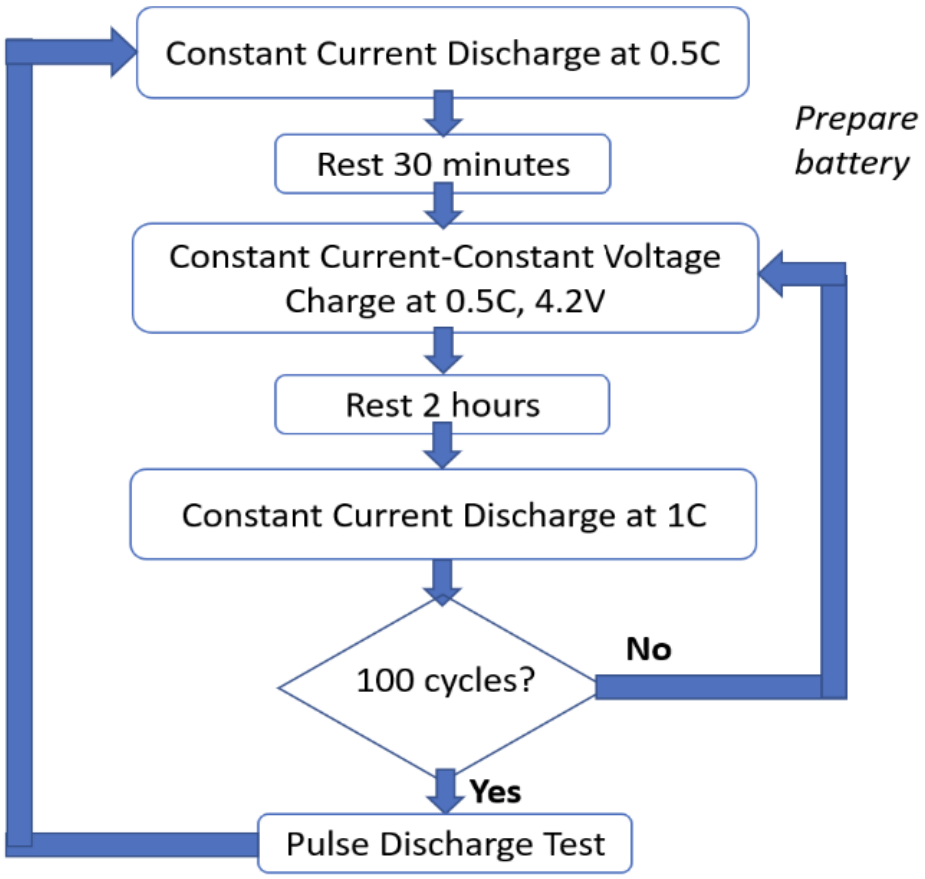

Figure 13. Battery cycling flowchart.

After repeating the test n times, which in this paper is kept at 100, a PDT is conducted on the battery to calculate its internal parameter values such as those mentioned in section C before continuing the cyclic tests.

The change in resistance of a HB used in cyclic ageing is compared to the resistance of a PESCB. This is done by resting the abused battery for an hour and then conducting a 10s pulse discharge test at 1C rate. The total internal resistance is calculated by summing up Ro, R1 and R2.

Internal resistance measurement

For parameter extraction, exponential curve fitting in Python is used. The collected data is fitted to the equation for a 2RC circuit. This circuit represents ohmic, electrochemical and concentration polarization of the battery [31]. The test profile used in this study consists of discharge pulses at different current values followed by a long rest period. Provided Ut is the battery terminal voltage, UOC is the open circuit voltage, Ro is the ohmic resistance, U1 and U2 are the voltages across the two RC circuits when current *I* is flowing, differential equations used for representing such a 2RC circuit are,

$$Ut = Uoc - I(t)Ro - U1 - U2 \quad (1)$$

$$\dot{U}1 = -\frac{U1}{R1C1} + \frac{I(t)}{C1} \quad (2)$$

$$\dot{U}2 = -\frac{U2}{R2C2} + \frac{I(t)}{C2} \quad (3)$$

Following the initial drop in the voltage due to ohmic polarization within the discharge pulse duration, electrochemical and concentration polarization start to occur and the data in this period can be fitted to [32]

$$Ut(t) = Uoc - IR1\left(1 - \left(e^{-\frac{t}{R1C1}}\right)\right) - IR2(1 - (e^{-\frac{t}{R2C2}})) \quad (4)$$

Data analysis

1. Extracting the OCV-SOC Curve:

- Battery is discharged at a very low current (typically C/20) to minimize internal heating and polarization effects.
- Battery voltage at regular intervals (e.g., every minute or every 1% drop in SOC) is recorded.
- Data smoothing is used to reduce noise in the recorded voltage data.
- A polynomial equation is fitted to the data to obtain the OCV-SOC relationship.

2. Identifying Ro, R1, R2, C1 and C2

- Pulse Discharge Test
- Current pulses of amplitude I, which can be 5A, 10A, 15A, 20A, 25A, 30A or 120A are applied, and the voltage drop from the beginning of the pulse to the end is recorded.
- Segment the voltage response into initial, middle, and final parts to isolate the effects of each circuit element.
- Calculate Ro
- Record the initial voltage before the pulse (U1) and the voltage immediately after the pulse is applied (U2).
- Calculate the series resistance using:

$$Ro = \frac{U1 - U2}{I}$$

3. Extracting RC Network Parameters (R1, C1, R2, C2)

- Subtract the immediate voltage drop due to Ro
- Inspect the remaining voltage segments, that is the middle and final part of the pulse and identify the exponential decay regions.

- Use curve fitting and curve fit the voltage data to equation 4 to obtain R1, C1, R2, and C2
- Use all the parameter values Ro, R1, R2, C1 and C2 to generate a voltage pulse using any open-source battery model.
- Compare the experimental and generated voltage data and minimize the error.

Code Snippets

- R2 versus Cycles plot:

```
"""
Created on Mon Mar 14 09:40:12 2022

@author: kaynat.zia
"""

import matplotlib.pyplot as plt
import pandas as pd
import numpy as np
import pandas as pd
import openpyxl
from openpyxl import load_workbook
from openpyxl.styles import Font
from openpyxl.chart import BarChart, Reference
import string



file_name_core_format = 'RPT_{} (2)'
rowj= 0
number_of_files=19
dtm1=[None] * number_of_files
dtm2=[None] * number_of_files
cycles=[0, 67, 134, 201, 268, 335, 402, 469, 536, 603, 670, 737, 779, 780, 847, 914, 915, 940, 996]
#cycles= [67] * number_of_files

for i in range(1, number_of_files+1):

    wb = load_workbook( file_name_core_format.format(i) + '.xlsx')
    sheet = wb.worksheets[0]
    dtm2[rowj]= sheet.cell(row=10, column=3).value
    rowj+=1
```

Dtm 2-dtm 10 are used for different SOC points. The above shown step is for 10% SOC and it's repeated for 20-90% SOC.

The code snippet shown below, takes the R1 values at every SOC point and plots it separately over the course of 1000 cycles. This is also repeated for Ro, R2 and R total.

```
cy=[0, 1]



plt.ylim([0.002, 0.027])
plt.plot(cycles, dtm2, color='gray', label= '10% SOC')
plt.plot(cycles, dtm3, color='red', label= '20% SOC')

plt.plot(cycles, dtm4, color='green', label= '30% SOC')

plt.plot(cycles, dtm5, color='yellow', label= '40% SOC')

plt.plot(cycles, dtm6, color='purple', label= '50% SOC')

plt.plot(cycles, dtm7, color='cyan', label= '60% SOC')

plt.plot(cycles, dtm8, color='magenta', label= '70% SOC')

plt.plot(cycles, dtm9, color='black', label= '80% SOC')

plt.plot(cycles, dtm10, color='blue', label= '90% SOC')
plt.legend(bbox_to_anchor = (1.05, 0.6))
plt.title('Polarization Resistance-2 Versus Cycles')
plt.xlabel('Cycles')
plt.ylabel('R2 (ohm)')
plt.show()




plt.legend(bbox_to_anchor = (1.05, 0.6))
```

- SOC:

```
# State of Charge
mean_current = 0.5*(initial_current + final_current)
coulombic_efficiency_frac
if mean_current >= 0:
    soc_frac[t] = soc_frac[t-1] + coulombic_efficiency_frac*mean_current*time_delta/capacity_As
else:
    soc_frac[t] = soc_frac[t-1] + (1/coulombic_efficiency_frac)*mean_current*time_delta/capacity_As
```

- Ro:

```
delta_current = np.diff( test_data['current_A'], prepend=test_data['current_A'][0] )
delta_voltage = np.diff( test_data['voltage_V'], prepend=test_data['voltage_V'][0] )

r0_values = delta_voltage[r0_key]/delta_current[r0_key]
```

This calculates DC resistance at every point of the discharge pulse. Later the maximum value is selected to be the Ro value for that SOC value. This is repeated for every SOC point and discharge rate.

- Tau1-Tau2:

```
rate_of_change = np.abs(np.diff(y) / np.diff(x))

# Identify the indices of the two highest rates of change
split_indices = np.argsort(rate_of_change)[-2:] + 1  # +1 to account for the diff shift

# Ensure the indices are in ascending order
split_indices.sort()

# Add start and end points for splitting
split_points = [0] + split_indices.tolist() + [len(x)]

# Split the curve into three parts
splits = [(x[split_points[i]:split_points[i+1]], y[split_points[i]:split_points[i+1]]) for i in range(len(split_points)-1)]
```

The discharge pulse is split into three parts based on the rate of change. The first part shows the ohmic properties whereas the last two parts represent the two polarization processes. The time constant Tau1 and Tau2 are calculated from the split discharge pulses. This information is later used to calculate R1-C1 and R2-C2.

Chapter 3: Results and discussion

A. Zero-bouncing during ESC

The setup discussed in this study is used to conduct ESCTs and since power MOSFETs are used instead of mechanical switching, no bouncing or glitching is spotted in the recorded data even when the sampling rate is as small as 500µs as seen in Fig. 14, which shows the terminal voltage across the battery terminals specifically during ESCTs at different SOC values. The discharge pulse period lasts for 10s, the discharge current smoothly spikes to its maximum value during the ESCT and then continues to decrease without interruption. As a result, the terminal voltage falls rapidly in the beginning of the test (proportional to the current spike) and then starts to fall gradually until the test is terminated for each of the SOC values (90%-20% with 10% increment) after 10s. The following observations are made upon inspecting the terminal voltage data with a naked eye:

1. cut-off voltage is reached sooner.
2. the battery depletes faster.
3. the rate of change of the terminal voltage is higher than during safe discharge levels.

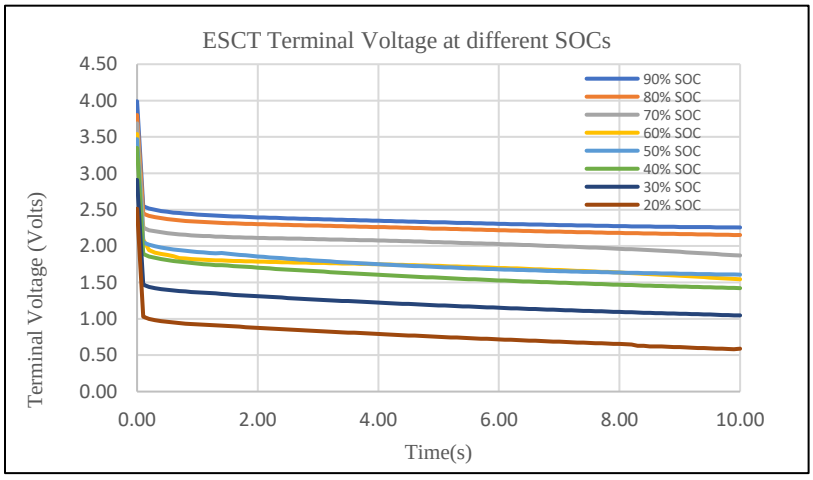

Figure 14. ESCT terminal Voltage Versus Time

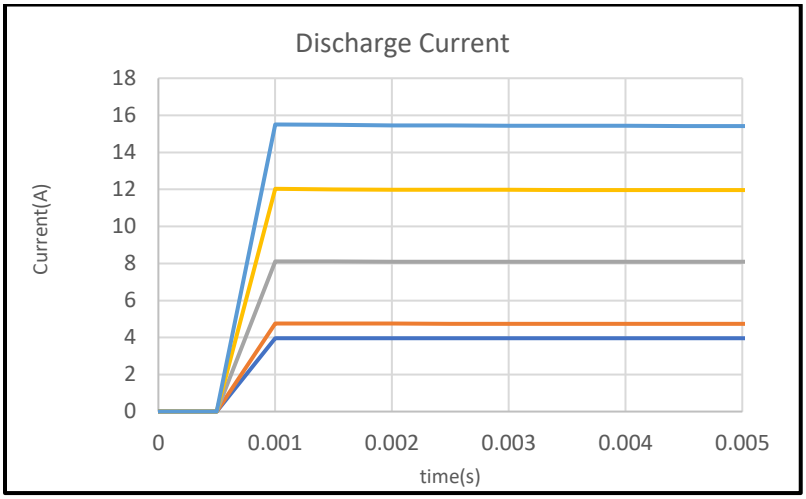

Figure 15. Discharge current in the first few milliseconds.

Even though the discharge period is short (10s), the battery is stressed out due to rapid discharging and releasing heat faster than it's removed from the body of the battery. If continued for longer, this kind of abuse testing can lead to thermal runaway. During thermal runaway the battery will release carcinogenic smoke, will go up in flames and expel ejecta. Thus, this kind of testing should be conducted in a controlled environment with proper PPE gear. This should include an enclosed fireproof chamber, a proper and clean exhaust fan for efficiently purifying the air being removed from the chamber, a fire extinguisher (water will work), cameras for visual inspection of the test subject etc. Gas masks, protective glasses, fireproof gloves etc. for the personnel handing over the abused battery is also necessary. This is why the duration of ESCTs was kept to 10s and 20s.

Figure 15 shows a zoom in of the current discharge pulse at various discharge rates. It's zoomed in to the first few milliseconds of the discharge to check for bouncing ang irregularities. The high

sampling rate provided by CRio, the fast-switching rate of the MOSFETs and the non-inductive nature of the resistors has contributed to the high quality of recorded data.

B. Battery parameters

The graphs in Figure 16-18. show the values of battery parameters calculated for a Ro-2RC-pair circuit across different values of SOC at the current values of 5, 10, 15, 20, 25, 30 and 120 Amps. These values are void of any moving/bouncing data due to the circuit design which has no moving parts. The values of these parameters also depend on the initial values chosen for (4) curve fitting, circuit elements and how long batteries were on the shelf post manufacturing and pre-test, among other factors.

It can be seen from these graphs that the curves representing Ro, R1 and R2 for 5-30 Amps have the same shapes. The parameter values extracted from 10s ESCT are, however, different apart from the values of Ro. The beginning of the ESCT discharge pulse or any discharge pulse that is going to last for 10s, is governed by the value of Ro, because it's quite early for the other processes like polarization to show up in the recorded data. In Fig. 8. it is seen that from 5 to 30Amps, the value of polarization resistance, R1, decreases overall across all SOC points, it's because the polarization processes are slow to start at low currents. For the discharge at 120 Amps, due to rapid polarization the value of R1 across all SOC points, increases instead of decreasing. For ESC R1 and ESC R2, the extracted data starts to divert from other entries at SOC below 70% (SOC<70%), as seen in Fig. 8 and Fig. 9 due to the polarization mentioned earlier. Secondly, it is due to over-discharge happening in the battery at lower SOC. As the SOC decreases, so does the open circuit voltage and the stored battery charge, that leads to the battery reaching its advised voltage cut-off of 2.5V sooner than it did at higher SOC values. Over-discharging of a battery can bring about capacity loss and irreversible structural damage such as

dendrite formation. However, the ESCT in this study is terminated at only 10s and the change in battery structure should not be significant. This is also supplemented by a lack of any visible signs of battery structure deterioration during testing. Thirdly, it can be attributed to the fact that a new battery cell is used for every ESCT conducted in this study instead of using an abused cell again. Figure 19 Shows a plot of total internal resistance of the battery at different C rates and SOC levels and the total resistance of the battery during ESCT is almost parallel to the total resistance at other C rates.

Before the batteries that were abused during the ESCTs, the PESCBs, are retired, they are used once more to calculate their total internal resistance. One PESCB was picked from the abuse tests which had undergone a 10 second ESCT at 70% SOC during the first phase of tests. A second, HB is taken, also brought to 70% SOC and has a 20s long ESCT conducted on it. Both the 10s and 20s ESCT are done at 70% SOC to ensure similar testing conditions. The internal resistance of both PESCBs is higher than their initial recorded resistance by at least 40%. Since battery resistance is different for every SOC point, resistances of these two PESCBs is compared with that of a cyclically aged battery, at each of the 8 (20-90%) SOC points, which is used as a point of reference.

Fig. 20-22 show the individual internal resistances, Ro, R1 and R2 across the increasing number of cycles of discharge for every SOC. Figure 24 shows the total internal resistance change across the cycles for every SOC plotted together so that variations across different SOC points can be seen, it can be seen from Fig. 25-40. that the resistance increase of a PESCB varies across every SOC point. Some SOC points show a higher increase in battery resistance than others. For example, at 80% SOC, the battery resistance recorded after both ESCT durations, is the highest. The smallest increase in resistance after a 10 second ESCT is observed at 30% SOC. It can be

seen from the graphs that the value of resistance increase is higher after a 20 second long ESCT than a 10s ESCT except at 90% SOC. Increase in the internal resistance of PESCB is not uniform and some SOC points show more resilience to the ESC abuse. Battery Management Systems can be configured to use such a battery within this range of SOC values. While both the batteries have significantly aged, they are in no way useless, instead they can be employed for short-term use to benefit from the remainder of their lifetime. Such PESCBs can be used for applications which don't require a very long battery life to prevent them from entering the waste stream [33]. Also, if the short circuit duration experienced by the battery is known, its resistance and remaining life can be estimated.

Another thing to be noted here is that the change in resistance, measured during 1000 lifecycles, follows its own trajectory across different SOCs. A side-by-side comparison can be seen in table 1. For the first battery, the number of cycles it would take a HB to reach this PESCB resistance are between 230 to more than 1000.

Studies like these should be conducted for batteries before use so there's data available when a battery undergoes an ESC. Based on the duration, temperature, SOC of the battery and the battery type a decision can be made about how to re-use the battery in the best possible way that is safe, environment friendly and cost-effective.

For future extension of this work, PESCBs should be cyclically aged to collect lifetime data that is unique to them. This will help study the impacts of ESC on a PESCB's performance, months and possibly years from the occurrence of ESC. Depending on the outcome, this contribution can help save more Li-ion batteries from early disposal and getting added to the e-waste.

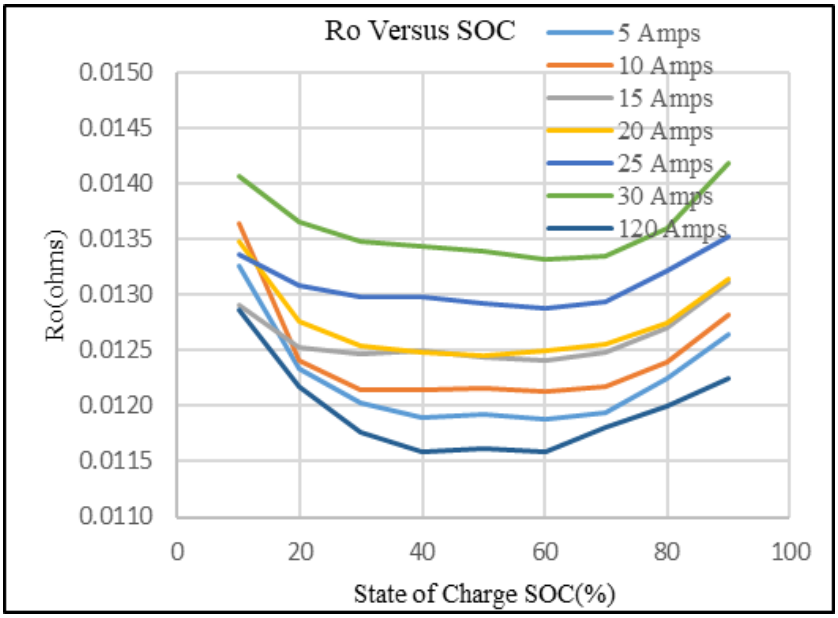

Figure 16. Ro versus SOC at different C rates.

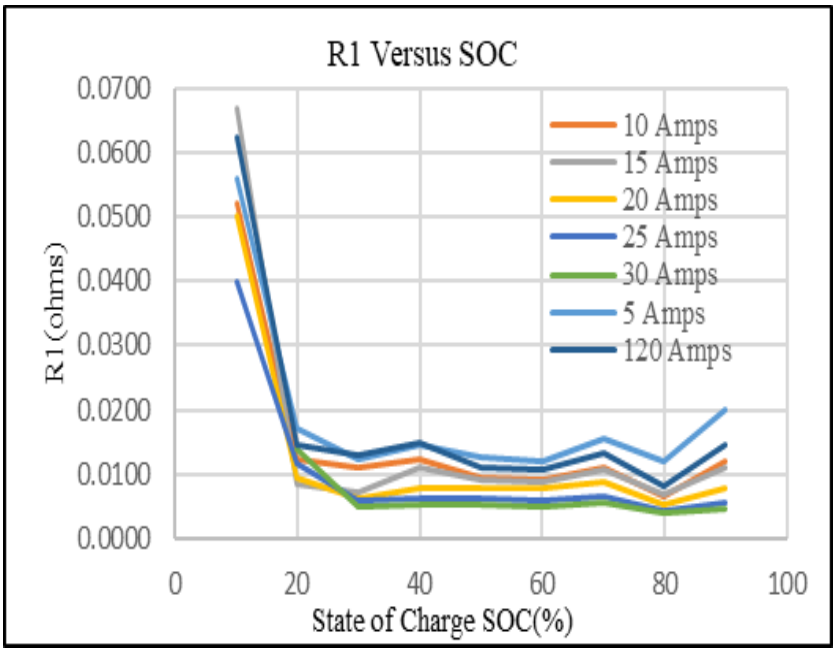

Figure 17. R1 versus SOC at different C rates.

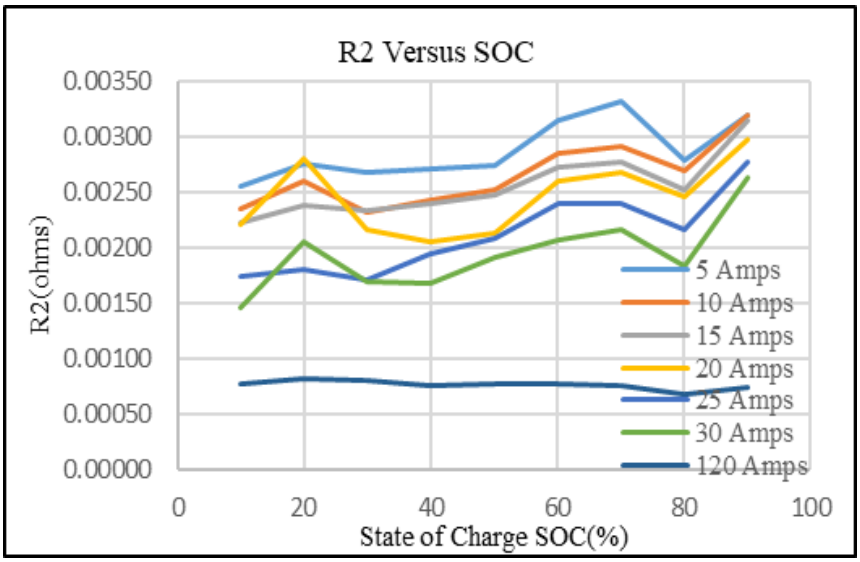

Figure 18. R2 versus SOC at different C rates.

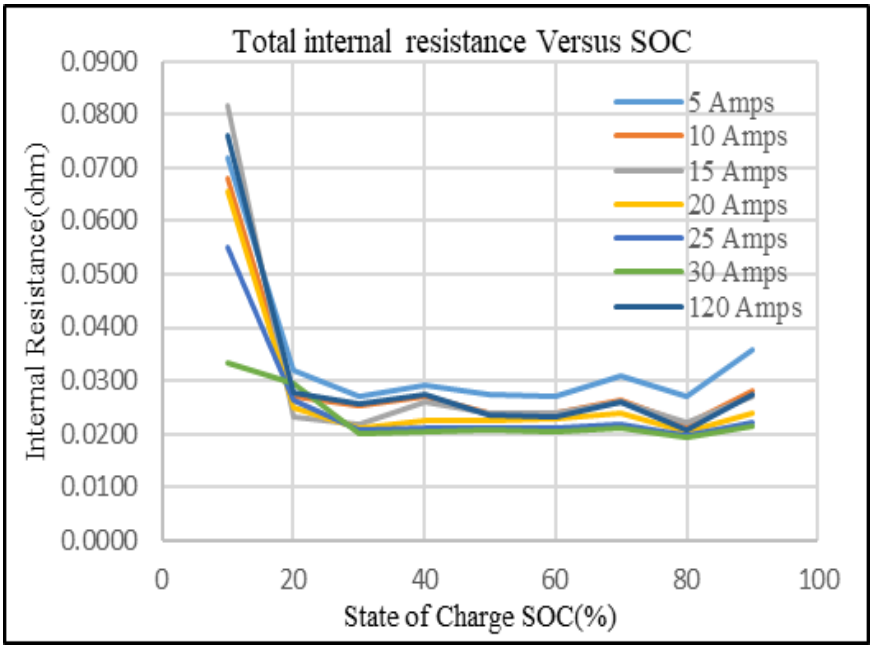

Figure 19. Total internal resistance of the battery at different C rates and SOC values.

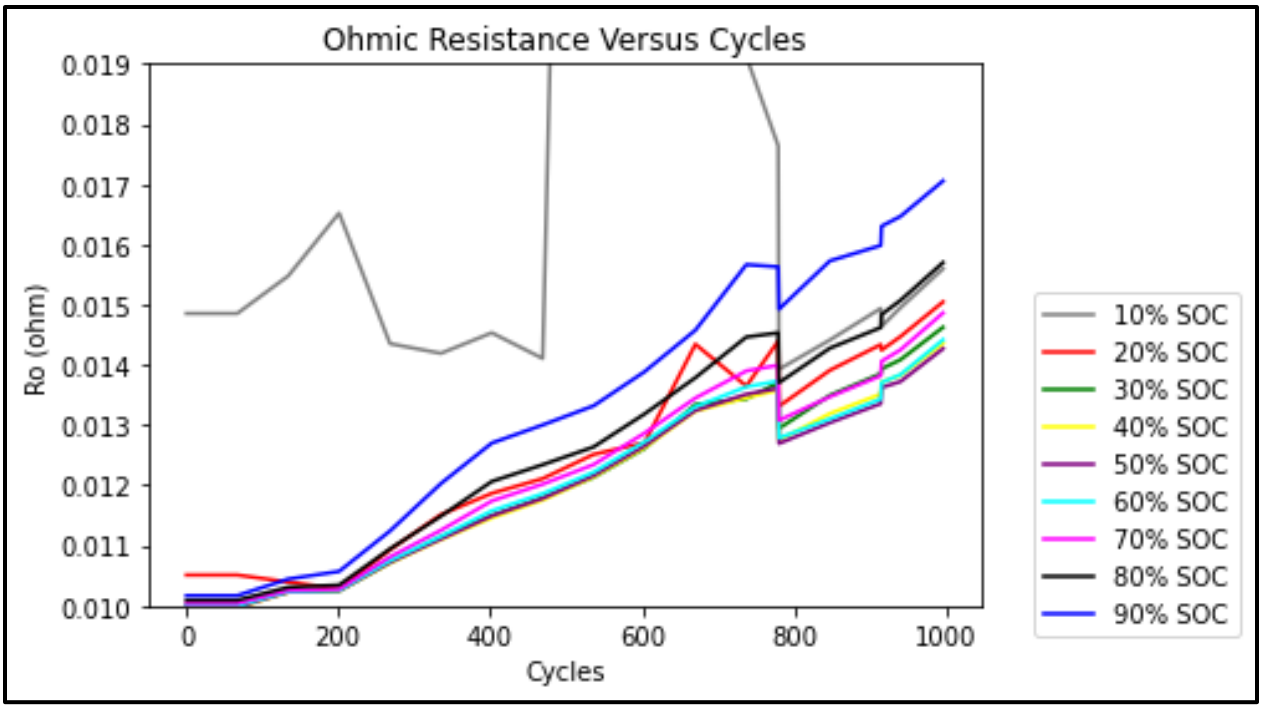

Figure 20. Ro Versus Battery Cycles

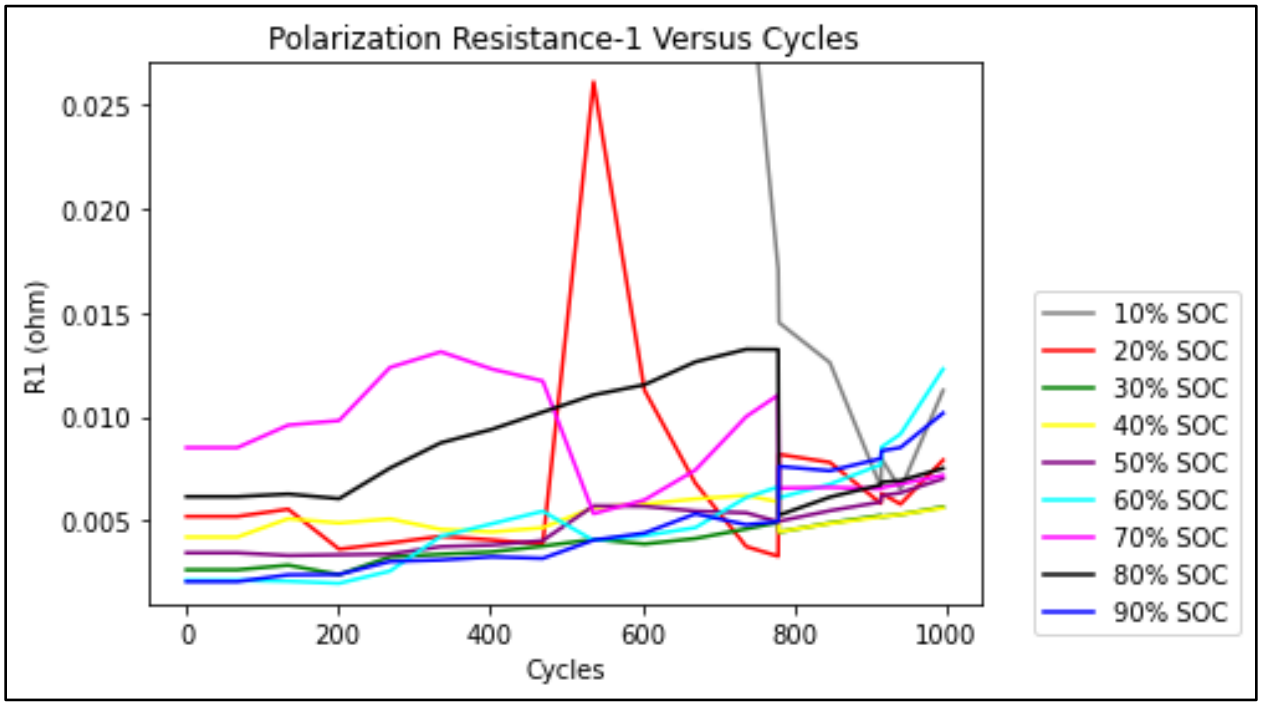

Figure 21. R1 versus battery cycles

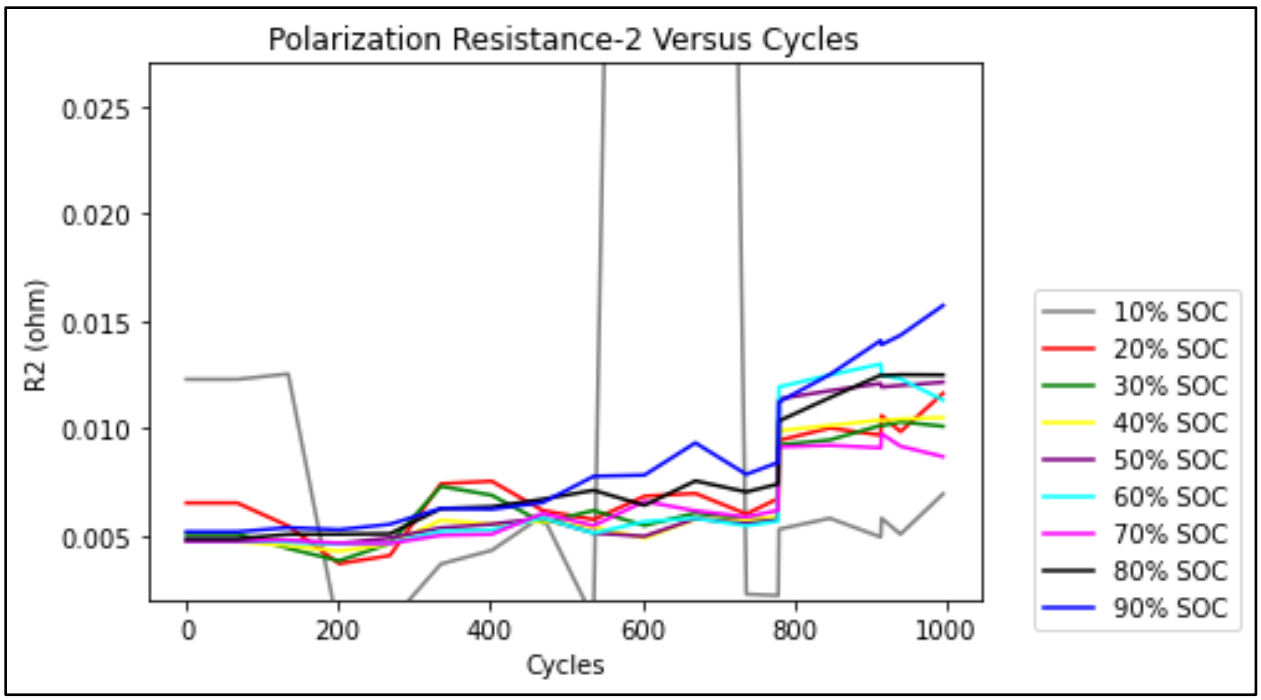

Figure 22. R3 versus battery cycles

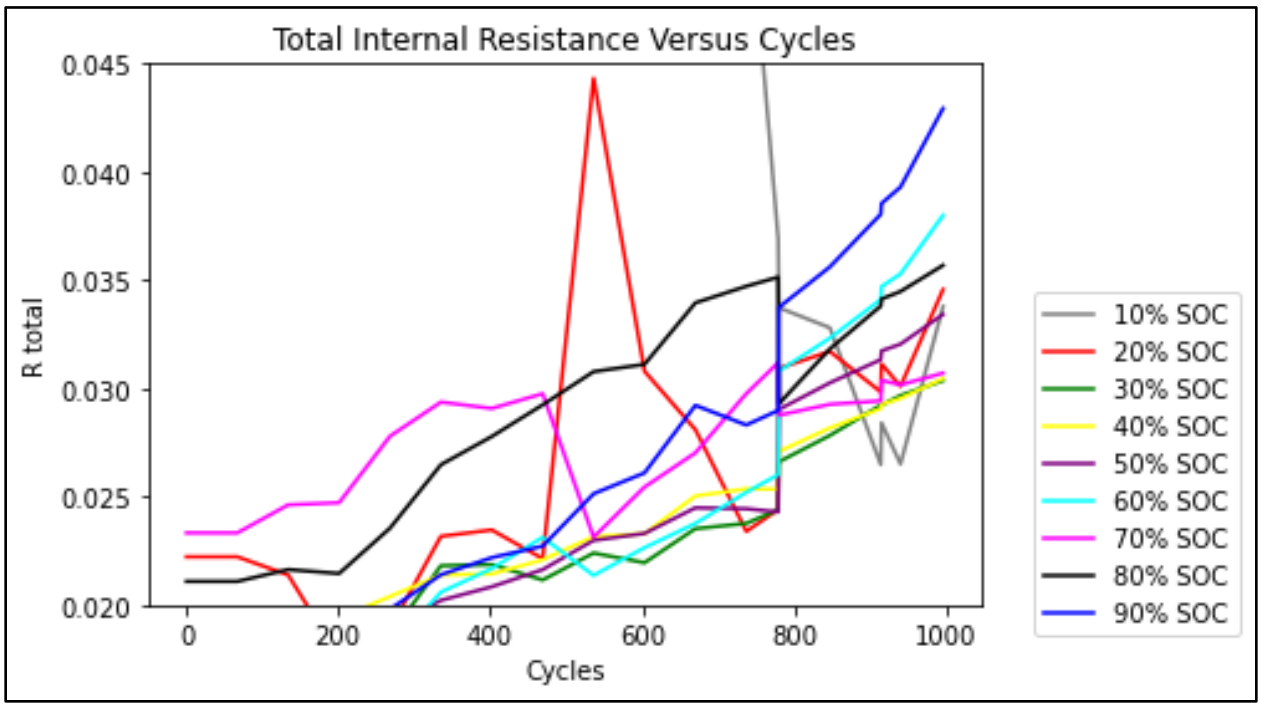

Figure 23. Total internal resistance versus battery cycles

The behavior of battery internal resistance at 10 and 20% SOC can be attributed to a number of things. From the chemical point of view, a significant portion of the lithium ions within the battery's cathode material have already been extracted and migrated towards the anode during discharge. This results in a lower concentration of lithium ions within the cathode i.e., reduced cathode potential, compared to higher SOC levels. Conversely, there is a higher concentration of lithium ions within the anode i.e., a higher anode potential. The Solid electrolyte Interphase (SEI) layer may have gone through changes due to electrochemical reactions happening such as pulse discharges, life cycling etc. low SOC levels, the concentration of lithium ions available for transport within the battery is reduced. This limitation in ion availability can result in slower ion transport kinetics, especially at the electrode-electrolyte interface.

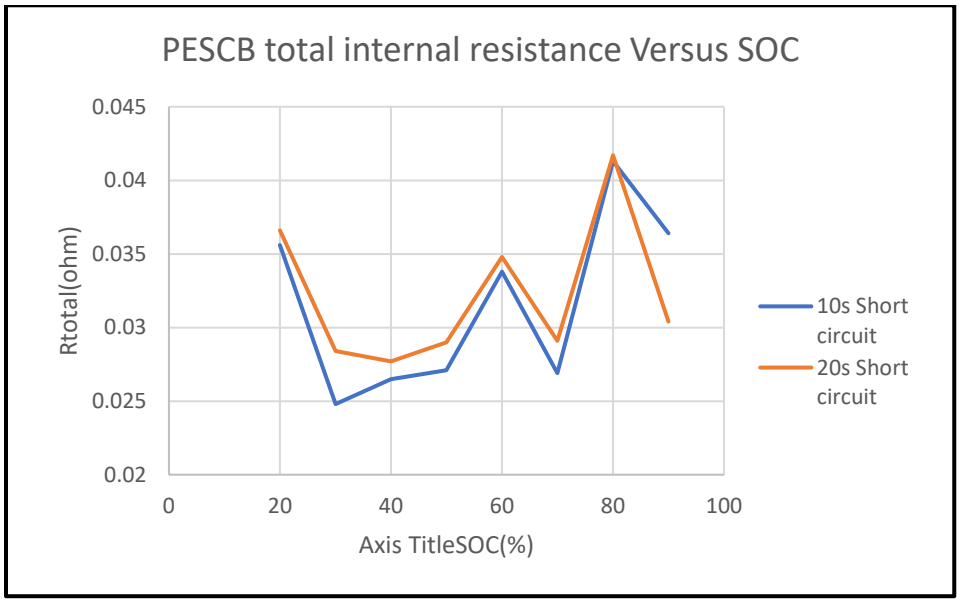

Figure 24.PESCB total internal resistance versus SOC

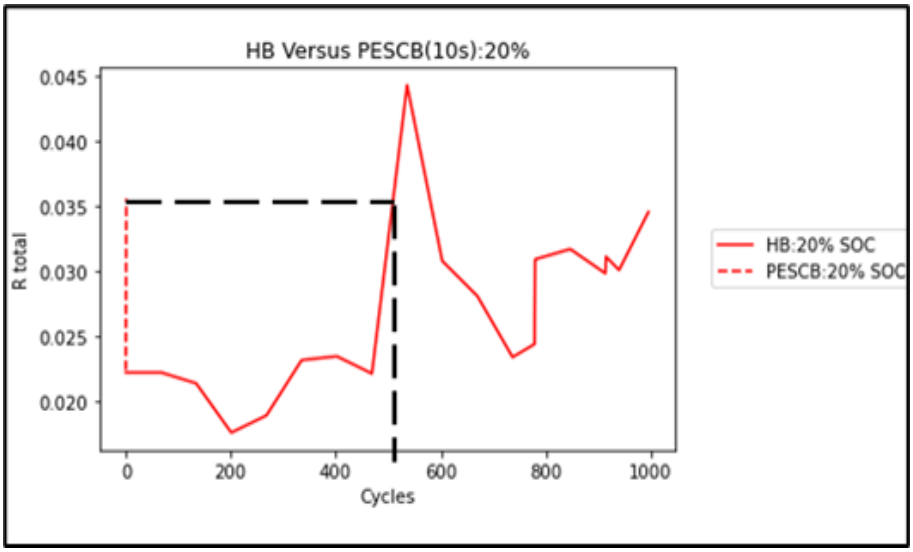

Figure 25. R total of a HB versus a PESCB (10s) at 20% SOC.

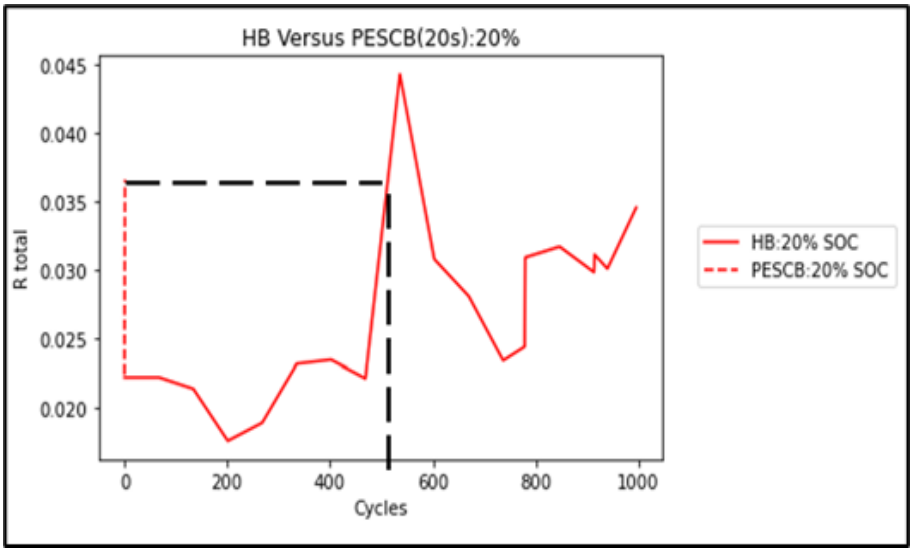

Figure 26. R total of a HB versus a PESCB (20s) at 20% SOC.

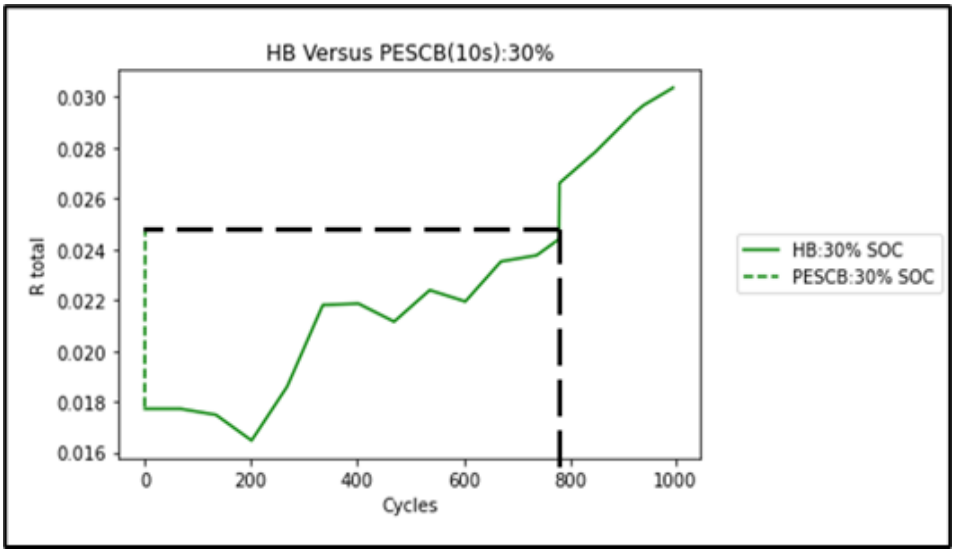

Figure 27. R total of a HB versus a PESCB (10s) at 30% SOC.

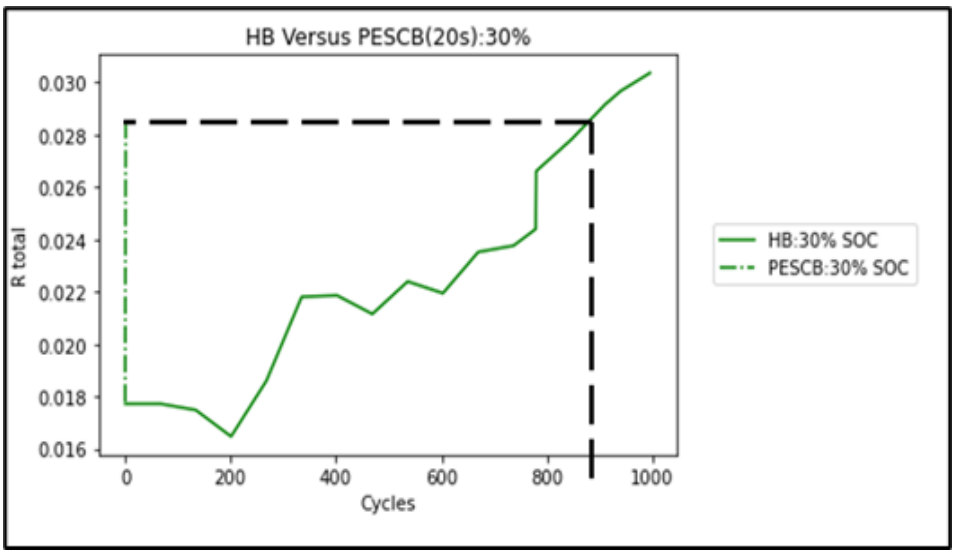

Figure 28. R total of a HB versus a PESCB (20s) at 30% SOC.

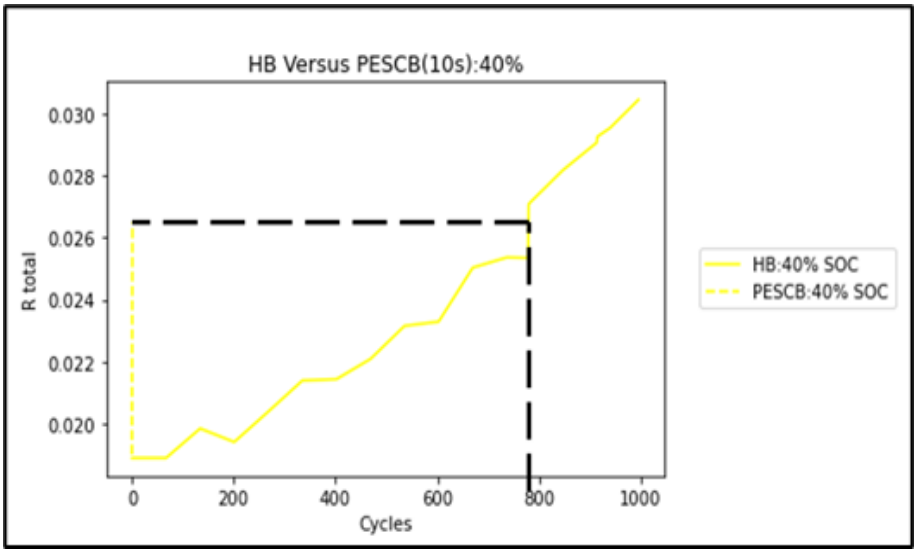

Figure 29. R total of a HB versus a PESCB (10s) at 40% SOC.

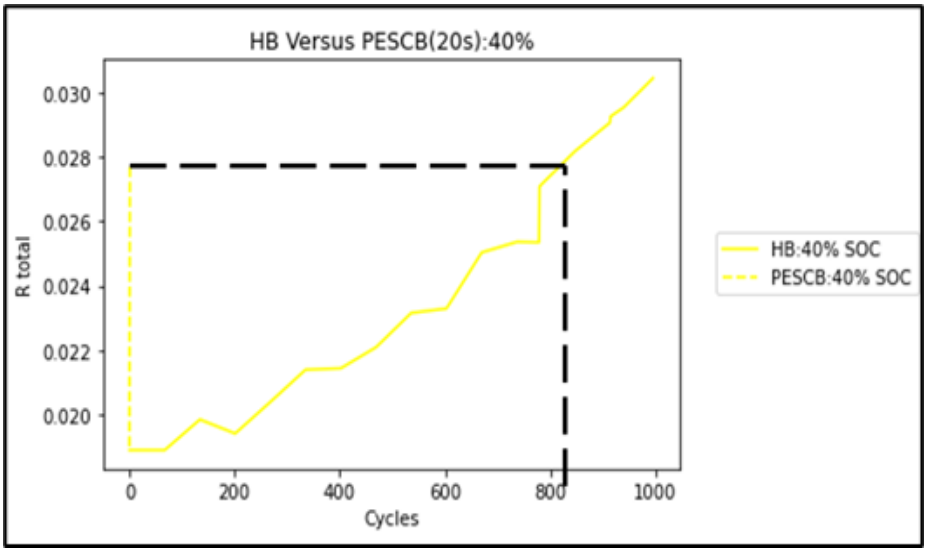

Figure 30. R total of a HB versus a PESCB (20s) at 40% SOC.

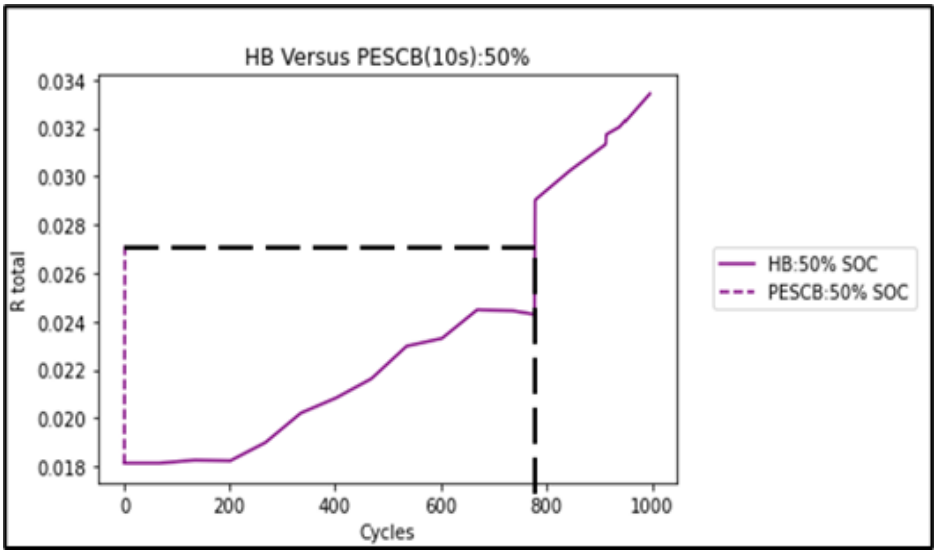

Figure 31. R total of a HB versus a PESCB (10s) at 50% SOC.

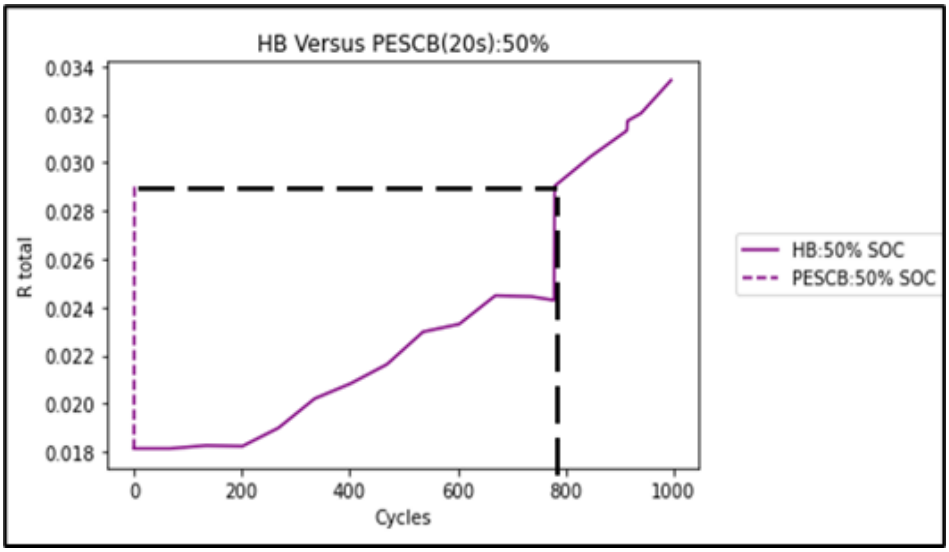

Figure 32. R total of a HB versus a PESCB (20s) at 50% SOC.

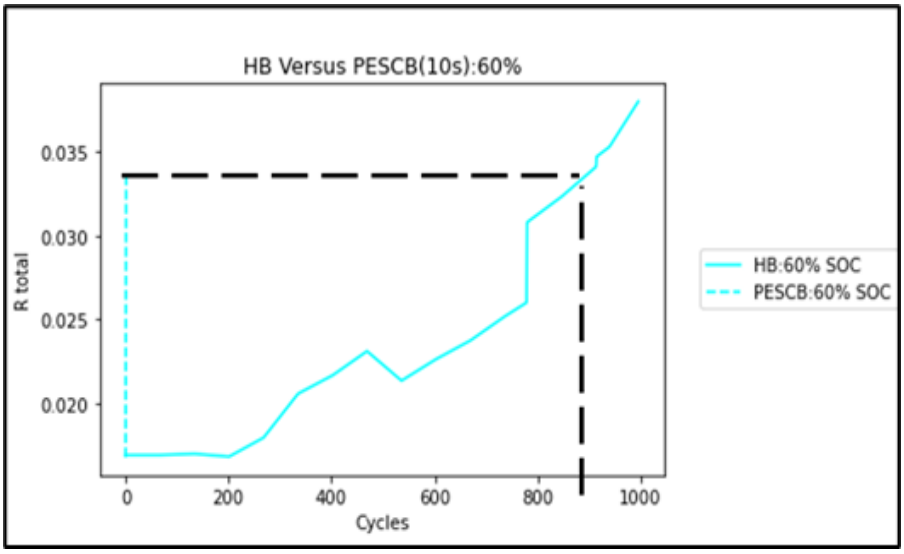

Figure 33. R total of a HB versus a PESCB (10s) at 60% SOC.

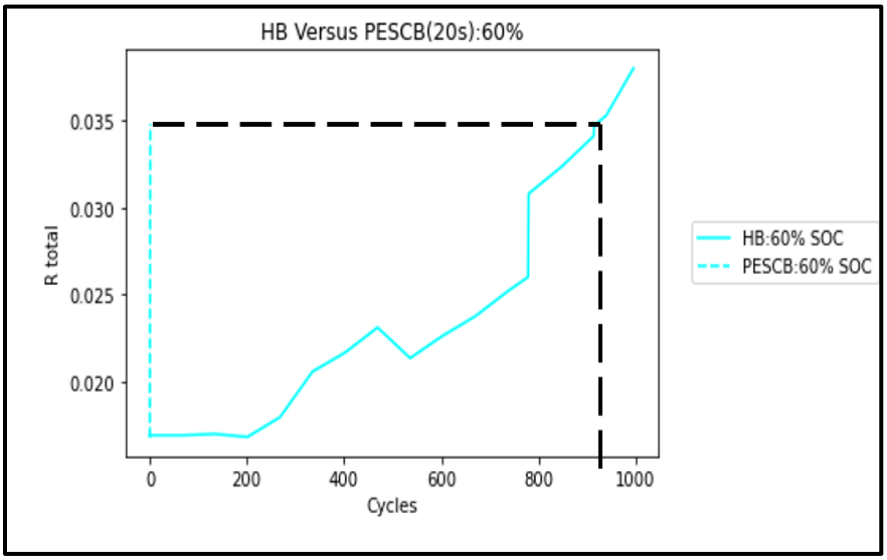

Figure 34. R total of a HB versus a PESCB (20s) at 60% SOC.

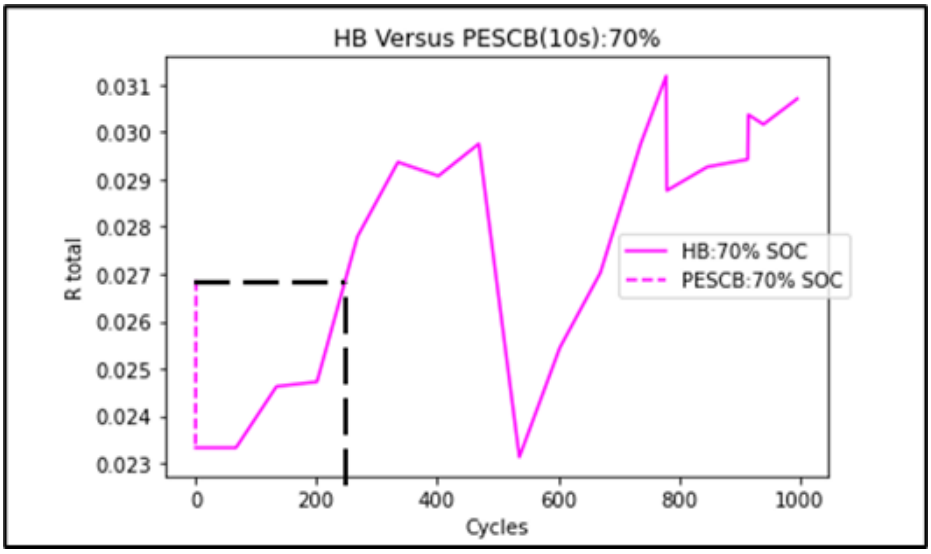

Figure 35. R total of a HB versus a PESCB (10s) at 70% SOC.

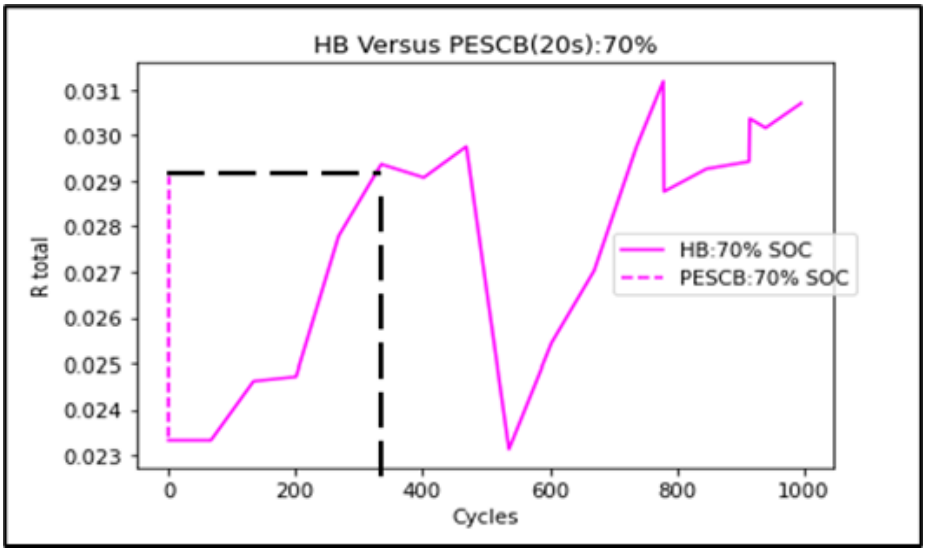

Figure 36. R total of a HB versus a PESCB (20s) at 70% SOC.

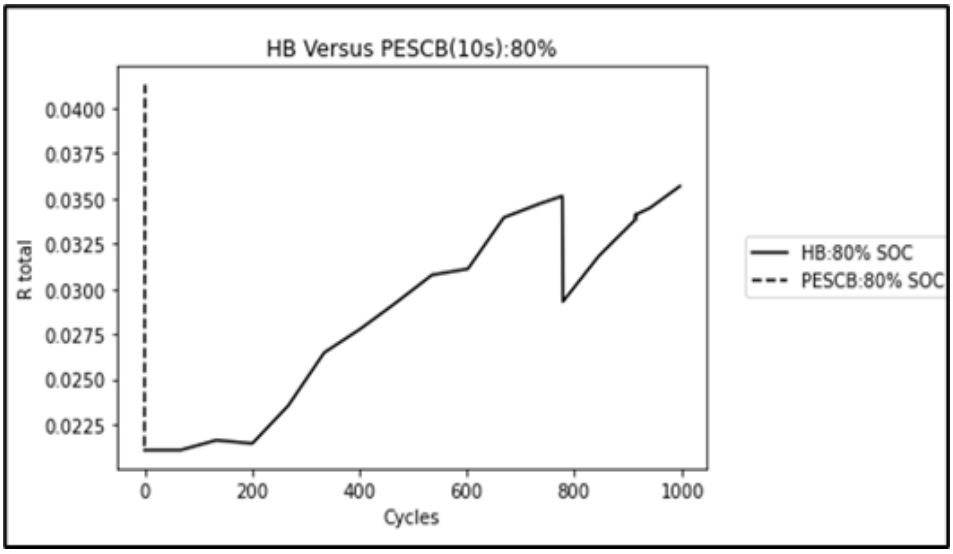

Figure 37. R total of a HB versus a PESCB (10s) at 80% SOC.

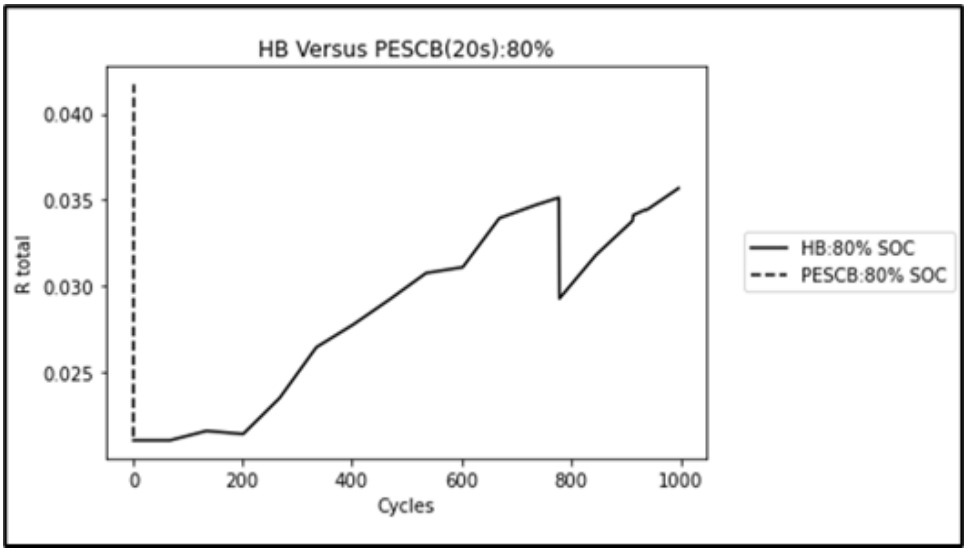

Figure 38. R total of a HB versus a PESCB (20s) at 80% SOC.

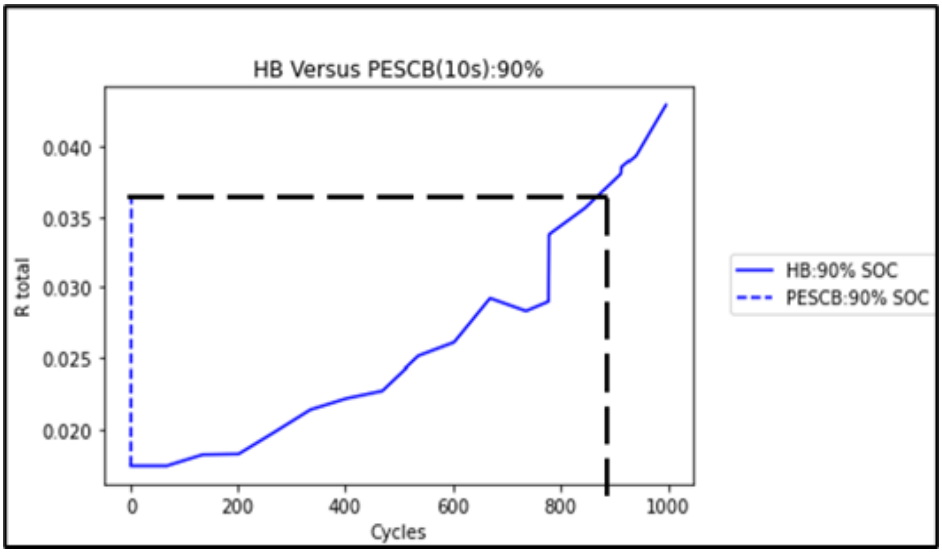

Figure 39. R total of a HB versus a PESCB (10s) at 90% SOC.

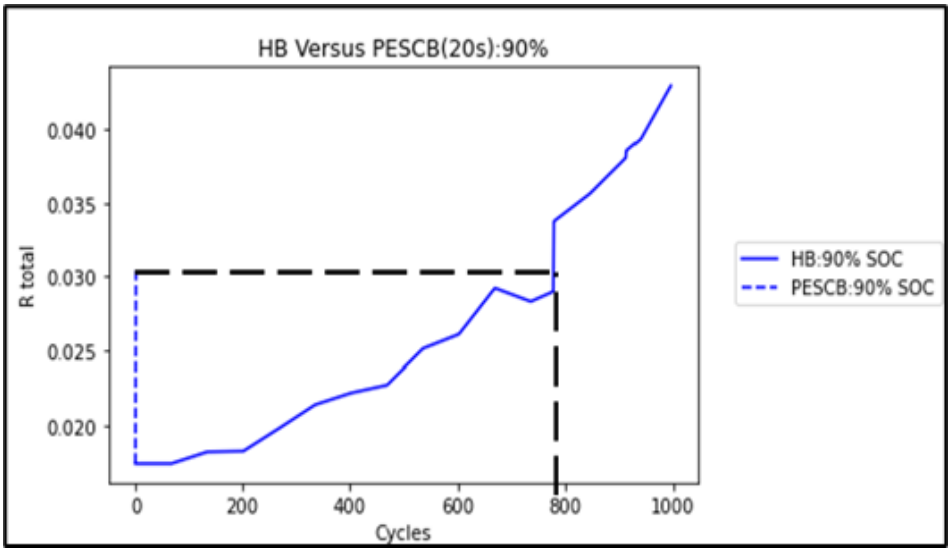

Figure 40. R total of a HB versus a PESCB (20s) at 90% SOC.

SOC	10s PESCB	Cycles	20s PESCB	Cycles
20	0.0356	500	0.0366	510
30	0.0248	780	0.0284	880
40	0.0265	780	0.0277	810
50	0.0271	780	0.029	790
60	0.0338	890	0.0348	910
70	0.0269	230	0.0291	330
80	0.0413	>1000	0.0417	>1000
90	0.0364	890	0.0304	790

Table 1. The number of cycles lost in a PESCB

It can be said that a PESCB's remaining life can be predicted based on the duration of the external short circuit. For instance, a PESCB after a 10s long external short circuit has a total internal resistance of 0.0271 at 40% SOC. A HB reaches this internal resistance at SOC% when it has been cycled for 780 cycles, never and never again. If the HB, is designed to be used for 1500 cycles at XC discharge rate, it still has about 720 cycles left and so on. The discharge rate used greatly determines the total useable cycles that an application can get out of a battery.

Chapter 4: Conclusion and future research

To conduct the ESCTs, a zero bouncing circuit was used. Zero bouncing means no bouncing or moving part in the entire system/ circuit as bouncing parts of the circuit can corrupt the recorded data for ESCTs. In ESCTs the high recorded current occurs in the first 1s. This current value obtained while conducting ESCTs is used to make intelligent circuits and battery protection mechanism and algorithms. As the occurring of bouncing and maximum short circuit current coincide, this is an undesirable feature of using moving parts in circuit such as switches or mechanical relays. This circuit used in this research employs switching, and control circuit made rout of MOSFETs instead. MOSFETS operate using magnetic fields which develop when the current flows through a coil, hence the moving and bouncing is entirely removed from the circuit. This can be seen from the recorded data shown in the previous chapter. MOSFETs used provide fast turn on times and turn off times, very low turn on resistance and are inexpensive. The load bank is made up of non-inductive resistors which are purely resistive in nature. Regular resistors have parasitic inductance which becomes very apparent at faster switching rates. Data acquisition and control is done using NI LabVIEW and CRio,

Battery parameters are extracted from the collected MPDT data, and it was seen that values of Ro, which are greatly responsible for the maximum value of ESC remain much the same as those recorded for a safe discharge current level. The polarization resistances, however, behaved differently for SOC values less than 70%.

PESCB and cyclically aged HB internal resistance change is compared, and it’s found that the resistance increases by a significant number of lifecycles in PESCB which varies across the SOC spectrum. Although the battery ages during an ESC, it can be employed for a less intensive application, in an effort to reduce LI-ION BATTERY waste.

Research questions.

This research concludes here but it rises many research questions and some of them are discussed below:

Cyclically aging the abused batteries:

It is discussed extensively in this project how an abused battery compares to a healthy but cyclically aged battery and how an abused battery is similar to normally ageing battery if the abusive is controlled in the early stages. This helps build a case for reusing PESCBs by plotting their characteristics onto the HB cycling data. There are a few unknowns here such as how will the PESCB fare if aged for 10s of 100s of cycles? By cyclically ageing different PESCBs, data about the future health of abused batteries can be collected which can help strengthen the case for reuse.

Best applications for abused batteries:

Batteries can be cyclically aged by using generic discharge profiles where the battery is discharged for a constant load or at 2C, 3C discharge rates etc based off the specification sheet or the manufacturer's recommendation. But in real life situations, that rarely is the case. A hairdryer or heater for instance would draw more energy in the beginning after it's switched on because it has to go from ambient to higher temperatures rapidly followed by a constant discharge until it's switched off.

Hence, both HBs and PESCBs should be tested for different dynamic discharge profiles to see what the best possible application of abused batteries can be.

Cyclic aging models for dynamic discharge:

While it's impossible to cyclically age a battery for every single existing application as it requires a lot of resources and one or them being time. It took a year to cyclically age the batteries used in this project to 1000 cycles. Models can be created to predict behaviors after collecting baseline data.

Different chemistries

While Li-ion batteries are far more prone to thermal runaway and fires in the events of extreme temperature, abusive conditions and accidents, many other battery chemistries including many lithium battery chemistries such as LiFePO4 are much safer. Going by this fact, more chemistries should be tested alongside Li-ion batteries to decide the best possible way to reuse them and when to discard them.

Future of batteries

The future of battery technology, both within and beyond lithium-ion systems, is poised for remarkable advancements that promise to revolutionize energy storage and sustainability. In the realm of Li-ion batteries, researchers are focused on enhancing energy density, enabling longer ranges for electric vehicles and extended battery life for portable electronics, as well as developing fast-changing technologies to significantly reduce recharge times. Solid-state Li-ion batteries, featuring solid electrolytes, offer increased safety, higher energy densities, and longer lifespans. Innovations in battery materials, such as silicon anodes and lithium-sulfur or lithium-air chemistries, are also being explored to further boost performance.

Beyond lithium-ion, alternative battery technologies are making strides. Solid-state batteries continue to be a focal point due to their superior safety and energy density. Sodium-ion batteries provide a cost-effective and abundant alternative, with ongoing improvements in performance.

Flow batteries, particularly vanadium redox flow batteries, are ideal for large-scale energy storage thanks to their scalability and durability. Metal-air batteries, like zinc-air and aluminum-air, are being developed for their high energy densities, suitable for long-duration storage needs. Additionally, bio-batteries and fuel cells are emerging as sustainable and efficient energy sources.

A critical aspect of these advancements is the emphasis on sustainability through improved recycling and reuse processes. As battery technologies evolve, so do methods for recycling spent batteries, recovering valuable materials, and minimizing environmental impact. Innovations in manufacturing processes aim to reduce the carbon footprint, while enhanced recycling techniques ensure that valuable resources are reclaimed and reused, contributing to a circular economy. These developments in battery technology, coupled with robust recycling initiatives, will not only improve performance and safety but also support a sustainable energy future.

References:

[1] Lv, S., Wang, X., Lu, W., Zhang, J., & Ni, H. (2021). The influence of temperature on the capacity of lithium ion batteries with different anodes. Energies, 15(1), 60. https://doi.org/10.3390/en15010060

[2] R.-H. Xiong and J. Li, “Terahertz transmission characteristics of free-standing fractal jesus-cross structure,” *Front. Phys*., vol. 8, 2020. doi:10.3389/fphy.2020.00023.

[3] Lubner, S., Kaur, S., Fu, Y., Battaglia, V., & Prasher, R. (2020). Identification and characterization of the dominant thermal resistance in lithium-ion batteries using operando 3-omega sensors. Journal of Applied Physics, 127(10). https://doi.org/10.1063/1.5134459

[4] Vilsen, S. B., Kær, S. K., & Stroe, D. (2020). Log-linear model for predicting the lithium-ion battery age based on resistance extraction from dynamic aging profiles. IEEE Transactions on Industry Applications, 56(6), 6937-6948. https://doi.org/10.1109/tia.2020.3020529

[5] Kim, D. H., Koo, K., Jeong, J. J., Goh, T., & Kim, S. W. (2013). Second-order discrete-time sliding mode observer for state of charge determination based on a dynamic resistance li-ion battery model. Energies, 6(10), 5538-5551. https://doi.org/10.3390/en6105538

[6] Li, Y., Liu, K., Foley, A., Zulke, A. A., Berecibar, M., Nanini-Maury, E., … & Hoster, H. E. (2019). Data-driven health estimation and lifetime prediction of lithium-ion batteries: a review. Renewable and Sustainable Energy Reviews, 113, 109254. https://doi.org/10.1016/j.rser.2019.109254

[7] K. Zhang et al., "An Early Soft Internal Short-Circuit Fault Diagnosis Method for Lithium-Ion Battery Packs in Electric Vehicles," in *IEEE/ASME Trans. Mechatron.*, vol. 28, no. 2, pp. 644-655, April 2023, doi: 10.1109/TMECH.2023.3234770.

[8] N. Yang, Z. Song, M. R. Amini, and H. Hofmann, “Internal short circuit detection for parallel-connected battery cells using convolutional neural network,” *Automot. Innov.*, vol. 5, no. 2, pp. 107–120, 2022. doi:10.1007/s42154-022-00180-6

[9] R.-H. Xiong and J. Li, “Terahertz transmission characteristics of free-standing fractal jesus-cross structure,” *Front. Phys*., vol. 8, 2020. doi:10.3389/fphy.2020.00023.

[10] G. D. Harper et al., “Roadmap for a sustainable circular economy in lithium-ion and Future Battery Technologies,” *J. Phys.: Energy*, vol. 5, no. 2, p. 021501, 2023. doi:10.1088/2515-7655/acaa57

[11] Secondary lithium-ion cells for the propulsion of electric road vehicles - Part 2: Reliability and abuse testing, IEC 62660-2, 2018.

[12] A. Rheinfeld, A. Noel, J. Wilhelm, A. Kriston, A. Pfrang, and A. Jossen, “Quasi-isothermal external short circuit tests applied to lithium-ion cells: Part I. measurements,” *J. Electrochem. Soc*., vol. 165, no. 14, 2018.

[13] B. Xia, Z. Chen, C. Mi, and B. Robert, “External Short Circuit Fault diagnosis for lithium-ion batteries,” presented at the *2014 IEEE Transp. Electrification Conf. and Expo (ITEC),* 2014.

[14] A. Kriston et al., “External Short Circuit performance of graphite-lini1/3co1/3mn1/3o2 and graphite-lini0.8co0.15al0.05o2 cells at different external resistances,” *J. Power Sources,* vol. 361, pp. 170–181, 2017.

[15] R. Yang, and R. Xiong, “On-board soft short circuit fault diagnosis of lithium-ion battery packs for electric vehicles using extended Kalman filter,” *CSEE J. Power Energy Syst.*, 2020.

[16] Z.-Y. Chen et al., “Benign-to-malignant transition in external short circuiting of lithium-ion batteries,” *Cell Rep.,* vol. 3, no. 6, p. 100923, 2022.

[17] R. Yang, R. Xiong, W. Shen, and X. Lin, “Extreme learning machine-based thermal model for lithium-ion batteries of electric vehicles under External Short Circuit,” *Engineering,* vol. 7, no. 3, pp. 395–405, 2021.

[18] R. Yang, R. Xiong, and W. Shen, “Experimental Study on External Short Circuit and overcharge of lithium-ion battery packs for Electric Vehicles,” presented at the *4th Int. Conf. Green Energy and Applications (ICGEA),* 2020.

[19] S. Okazaki, S. Higuchi, N. Kubota, and S. Takahashi, “Measurement of short circuit current for low internal resistance batteries,” *J. Appl. Electrochem.*, vol. 16, no. 4, pp. 513–516, 1986.

[20] J.-B. Jung, M.-G. Lim, J.-Y. Kim, B.-G. Han, B. Kim, and D.-S. Rho, “Safety Assessment for External Short Circuit of Li-Ion Battery in ESS Application Based on Operation and Environment Factors,” *Energies,* vol. 15, no. 14, p. 5052, Jul. 2022, doi: 10.3390/en15145052.

[21] W. Liu, T. Placke, and K. T. Chau, “Overview of batteries and battery management for Electric Vehicles,” *Energy Rep.,* vol. 8, pp. 4058–4084, 2022. doi:10.1016/j.egyr.2022.03.016

[22] R. Xiong, S. Ma, H. Li, F. Sun, and J. Li, “Toward a safer battery management system: A critical review on diagnosis and prognosis of battery short circuit,” *iScience,* vol. 23, no. 4, p. 101010, 2020. doi:10.1016/j.isci.2020.101010

[23] K. Nováková, A. Pražanová, D.-I. Stroe, and V. Knap, “Second-life of lithium-ion batteries from electric vehicles: Concept, aging, testing, and applications,” *Energies,* vol. 16, no. 5, p. 2345, 2023. doi:10.3390/en16052345

[24] E. Redondo-Iglesias, P. Venet, and S. Pelissier, “Modelling lithium-ion battery ageing in Electric Vehicle Applications—calendar and cycling ageing combination effects,” *Batteries,* vol. 6, no. 1, p. 14, 2020.

[25] J. Mulqueen, “Inductive vs. non-inductive resistors,” forum.digikey.com, https://forum.digikey.com/t/inductive-vs-non-inductive-resistors/62. (Accessed Nov 16, 2021).

[26] “Take your first measurement in labview real-time (data logging),” NI, https://knowledge.ni.com/KnowledgeArticleDetails?id=kA03q000000x0UdCAI&l=en-US (accessed Jul. 25, 2024).

[27] M.-K. Tran et al., “A comprehensive equivalent circuit model for lithium-ion batteries, incorporating the effects of state of health, state of charge, and temperature on model parameters,” Journal of Energy Storage, vol. 43, p. 103252, Nov. 2021, doi: 10.1016/j.est.2021.103252.

[28] S. Barcellona, S. Colnago, G. Dotelli, S. Latorrata, and L. Piegari, “Aging effect on the variation of Li-ion battery resistance as function of temperature and state of charge,” Journal of Energy Storage, vol. 50, p. 104658, Jun. 2022, doi: 10.1016/j.est.2022.104658.

[29] J. Tinnemeyer and Z. Carlin, “Pulse-discharge battery testing methods and apparatus,” U.S. Patent 20080024137A1, Aug. 14, 2006.

[30] A. Barai, G. H. Chouchelamane, Y. Guo, A. McGordon, and P. Jennings, “A study on the impact of lithium-ion cell relaxation on electrochemical impedance spectroscopy,” *J. Power Sources*, vol. 280, pp. 74–80, 2015.

[31] K. Huang, Y. Wang, and J. Feng, “Research on equivalent circuit model of lithium-ion battery for electric vehicles,” presented at the *3rd World Conf. Mechanical Engineering and Intelligent Manufacturing (WCMEIM)*, 2020.

[32] C. Liao, H. Li, and L. Wang, “A dynamic equivalent circuit model of Lifepo4 cathode material for lithium-ion batteries on Hybrid Electric Vehicles,” presented at the *IEEE Vehicle Power and Propulsion Conf.*, 2009.

[33] K. Richa, C. W. Babbitt, G. Gaustad, and X. Wang, “A future perspective on lithium-ion battery waste flows from Electric Vehicles,” *Resour. Conserv. Recycl.*, vol. 83, pp. 63–76, 2014.